

1

Metal-Organic Framework Materials

Cameron J. Kepert

School of Chemistry, The University of Sydney, Sydney NSW, Australia

1.1 INTRODUCTION

In recent years there has been a rapid growth in the appreciation of molecular materials not just as arrangements of discrete molecular entities, but as infinite lattices capable of interesting cooperative effects. This development has arisen on many fronts and has seen the emergence of chemical and physical properties more commonly associated with non-molecular solids such as porosity, magnetism, and electrical conductivity. This chapter focuses on an area of molecular materials chemistry that has seen an extraordinarily rapid recent advance, namely, that of metal-organic frameworks (MOFs).[†] These materials consist of the linkage of metal ions or metal ion clusters through coordinative bridges to form

[†] Whilst certain qualifications on the use of the term ‘metal-organic framework’ have been put forward (*e.g.*, relating to formal bond valence and energy, ligand type, *etc.*),^[3] the common usage of this term has spread well beyond these to become largely interchangeable with a number of more general terms such as ‘coordination polymer’, ‘coordination framework’, ‘metallo-supramolecular network’ and ‘hybrid material’. As such, this term is used here, with some reluctance, in its broadest general sense to encompass a very diverse range of material types in which metal atoms are linked by molecular or ionic ligands.

frameworks that may be one-dimensional (1D), two-dimensional (2D) or three-dimensional (3D) in their connectivity.^[1–14]

In the broadest sense, the use of coordination chemistry to produce framework materials has been with us since the discovery of Prussian Blue more than 300 years ago, with developments throughout the last century providing an array of framework lattices spanning a range of different ligand types.^[15, 16] The rapid expansion of this early work into more structurally sophisticated families of materials can be traced to two developments. First, the exploitation of the strong directionality of coordination bonding has allowed a degree of materials design (so-called ‘crystal engineering’) in the synthesis of framework phases. Here, the use of molecular chemistry has allowed both the rational assembly of certain framework topologies – many not otherwise accessible in the solid state – and the control over framework composition through the incorporation of specific building units in synthesis or through post-synthetic modification. Secondly, the capability to construct materials in a largely predictive fashion has led to the emergence of a range of new properties for these materials. This most notably includes porosity, as seen in the ability to support extensive void micropore volume, to display high degrees of selectivity and reversibility in adsorption/desorption and guest-exchange, and to possess heterogeneous catalytic activity. A range of other interesting functionalities have also emerged, many in combination with reversible host–guest capabilities. A particularly attractive feature of the metal-organic approach to framework formation is the versatility of the molecular ‘tool-box’, which allows intricate control over both structure and function through the engineering of building units prior to and following their assembly. The adoption of this approach has been inspired in part by Nature’s sophisticated use of molecular architectures to achieve specific function, spanning host–guest (*e.g.* ion pumping, enzyme catalysis, oxygen transport), mechanical (*e.g.* muscle action), and electronic (*e.g.* photochemical, electron transport) processes. Following rapid recent developments the immensely rich potential of MOFs as functional solids is now well recognised.

At the time of writing this field is experiencing an unprecedented rate of both activity and expansion, with several papers published per day and a doubling in activity occurring every *ca* 5 years. Faced with this enormous breadth of research, much of which is in its very early stages, the aim of this chapter is not to provide an exhaustive account of any one aspect of the chemistry of MOFs, rather, to provide a perspective of recent developments through the description of specific representative examples, including from areas yet to achieve maturity. Following a broad overview of the host–guest chemistry of these materials in Section 1.2, particular

focus is given to the incorporation of magnetic, electronic, optical, and mechanical properties in Section 1.3.

1.2 POROSITY

1.2.1 Framework Structures and Properties

1.2.1.1 Design Principles

1.2.1.1.1 Background

The investigation of host–guest chemistry in molecular lattices has a long history. Following early demonstrations of guest inclusion in various classes of molecular solids (*e.g.* the discovery of gas hydrates by Davy in 1810), major advances came in the mid twentieth century with the first structural rationalisations of host–guest properties against detailed crystallographic knowledge. Among early classes of molecular inclusion compounds to be investigated for their reversible guest-exchange properties were discrete systems such as the Werner clathrates and various organic clathrates (*e.g.* hydroquinone, urea, Dianin’s compound, *etc.*), in which the host lattices are held together by intermolecular interactions such as hydrogen bonds, and a number of framework systems (*e.g.* Hofmann clathrates and the Prussian Blue family), in which the host lattices are constructed using coordination bonding.^[15, 16] A notable outcome from this early work was that the host–guest chemistry of discrete systems is often highly variable due to the guest-induced rearrangement of host structure, and that the coordinatively linked systems – in particular those with higher framework dimensionalities – generally display superior host–guest properties with comparatively higher chemical and thermal stabilities on account of their higher lattice binding energies.

Whilst the excellent host–guest capabilities of coordinatively bonded frameworks have been appreciated for many decades, the extension of this strategy to a broad range of metals, metalloligands and organic ligands has been a relatively recent development. Concerted efforts in this area commenced in the 1990s following the delineation of broad design principles^[1] and the demonstration of selective guest adsorption;^[17] notably, these developments arose in parallel with the use of coordination bonds to form discrete metallosupramolecular host–guest systems.^[18] A number of different families of coordinatively bridged material have since been developed, each exploiting the many attractive features conferred by the

coordination bond approach. A consequence of this rapid expansion is that many inconsistencies have arisen in the terminology used to distinguish these various families. In this chapter, the broadest and arguably most fundamental distinction, *i.e.* the exploitation of coordination bonding to form frameworks consisting of metal ions and molecular or ionic ligands, is used to define this diverse class of materials.

1.2.1.1.2 MOF Synthesis

In comparing MOFs with other classes of porous solids many interesting similarities and points of distinction emerge. A comparison has already been made above with discrete inclusion compounds, for which it was noted that coordinative rather than intermolecular linkage confers a high degree of control over materials' structure and properties, whilst retaining the benefits associated with the versatility of molecular building units. At the other end of the spectrum, an equally useful comparison can be made with other porous framework materials, which notably include zeolites and their analogues (*e.g.* AlPOs). Here, some close parallels exist between the structural behaviours of the host lattices, but many important differences exist relating to synthesis, structure and properties. One principal point of distinction is that the building units of MOFs are commonly pre-synthesised to a high degree. This allows the achievement of specific chemical and physical properties through a highly strategic multi-step synthesis in which the comparatively complex structure and function of the molecular units are retained in the framework solid. This ability to retain the structural complexity of the covalent precursors is a direct result of the low temperature synthesis of MOFs (*i.e.* typically <100 °C, with the majority able to be performed at room temperature), which in turn may be attributed to the favourable kinetics of framework formation; whereas the synthesis of more conventional porous framework solids commonly requires high temperatures, the labile nature of the metal-ligand bond in solution means that MOF assembly with error-correction can occur at low temperatures and over nongeological time periods to produce highly crystalline, ordered structures. As such, whereas the achievement of structural metastability and complexity in zeolites is generally achieved through control of the kinetics of framework formation or through framework templation and subsequent calcination, for MOFs a high degree of complexity is intrinsic to the molecular building units and can thus be achieved to a large extent through thermodynamic control.

There are two important further consequences of the low temperature route to framework formation. First, the entropic penalty associated with

the entrapment of solvent in channels and pores is less pronounced than for higher temperature synthetic routes. Secondly, and conversely, the enthalpic favourability of regular bond formation is a dominant driving force for framework formation. Through exploitation of the highly directional nature of coordination bonding, a reasonable degree of control over the structure of MOF lattices can thus be achieved. Extensive efforts in the use of well defined coordination geometries and suitably regular ligands have led to the development of relatively sophisticated ‘crystal engineering’ principles, albeit with absolute control over polymorphism in many cases being subject to the whims of crystal nucleation and subtle sensitivities to temperature, solvent, *etc.*

Among a range of useful design principles for MOFs are the ‘node and spacer’^[19, 20] and reticular ‘secondary building unit’ (SBU)^[21, 22] approaches. Common to each of these is the concept of using multitopic ligands of specific geometry to link metal ions or metal ion clusters with specific coordination preferences. Using these approaches it is possible to distill framework formation to the generation of networks of varying topology[‡]^[23–28] with the geometry of these being determined in large part by the geometry of the molecular building units (see Figure 1.1). In many cases the geometry of the building units defines a single possible network topology if fully bonded; for example, the use of octahedral nodes and equal-length linear linkers generates the cubic α -Po network [see Figure 1.1(i)]. In many cases, however, only the dimensionality of the resulting framework can be predicted with any reasonable degree of certainty, with very low energy differences arising due to torsional effects, intraframework interactions or subtle geometric distortions; for example, the use of tetrahedral nodes and linear linkers can generate a range of 3D 4-connected nets that include cristobalite [diamondoid; Figure 1.1(f)], tridymite (lonsdaleite), and quartz. In many further cases still, even the prediction of network dimensionality is not straightforward; for example, square nodes and linear linkers can produce a 2D square grid and a 3D NbO-type net [Figure 1.1(e) and (h)], and triangular nodes and linear linkers can produce a wide range of nets that vary only in their torsional angles through the linear linkers, *e.g.*, 0° torsion produces the hexagonal (6,3)

[‡]A large number of different chemical classification systems exist for network topologies. These notably include those based on simple chemical compounds (*e.g.* diamondoid/cristobalite-type), an (n,p) system used by Wells related to that of Schläfli that classifies according to the number of links in a loop (n) and the node connectivity (p) [*e.g.* (6,4)],^[23] a three-letter system derived from that used for zeolites (*e.g.* dia, dia-a, dia-b, *etc.*),^[24] and a 2D hyperbolic approach (*e.g.* sqc6).^[25] As an example, the chiral (10,3)-a network is known also as the SrSi₂ net, srs, Laves net, Y*, 3/10/c1, K4 crystal, and labyrinth graph of the G surface.

net, 109.5° torsion produces the chiral (10,3)-a net [see Figure 1.1(a–c)], *etc.* A further point of considerable complication from a design perspective is the interpenetration of networks,^[27] which has a profound influence over the pore structure and therefore host–guest properties.

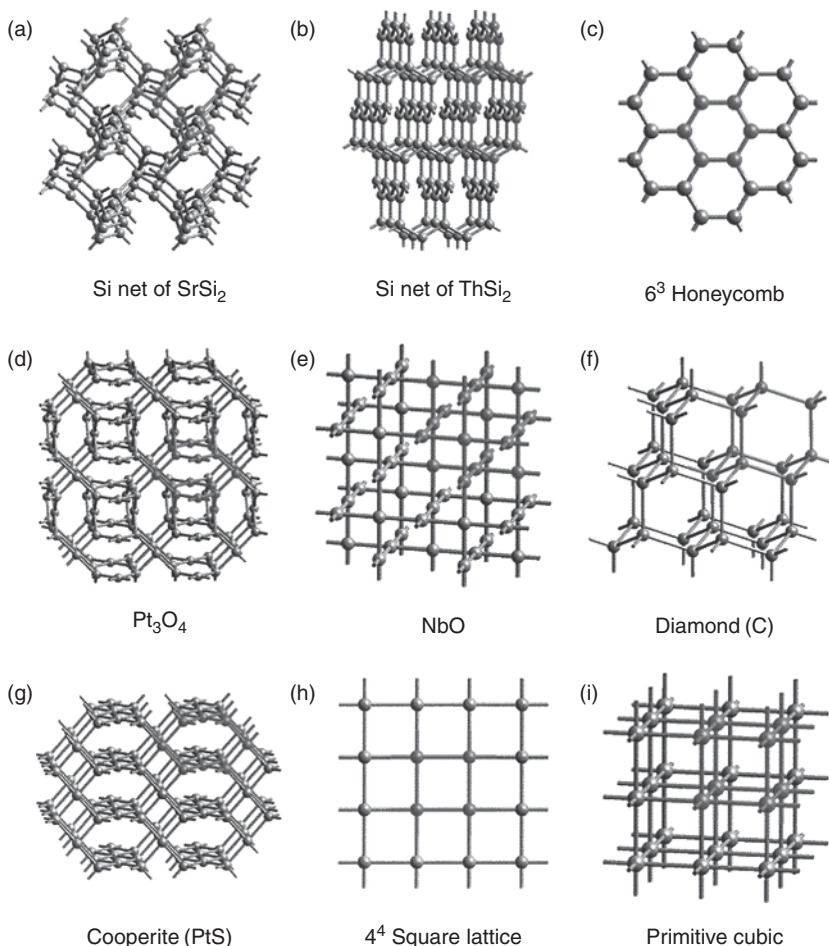


Figure 1.1 A selection of common network topologies for MOFs: (a) the 3-connected SrSi_2 [also (10,3)-a] net, shown distorted away from its highest symmetry; (b) the 3-connected ThSi_2 net; (c) the 2D hexagonal grid; (d) the Pt_3O_4 net, which contains square planar and trigonal nodes; (e) the NbO net, which contains square planar nodes; (f) the diamondoid net; (g) the PtS net, which contains tetrahedral and square planar nodes; (h) the 2D square grid; and (i) the α -Po net. Reprinted with permission from M. Eddaoudi, D.B. Moler, H.L. Li, B.L. Chen, T.M. Reineke, M. O’Keeffe and O.M. Yaghi, *Acc. Chem. Res.*, **34**, 319. Copyright (2001) American Chemical Society

An important consequence of both the versatility of the molecular building units and the accessibility of novel framework topologies is that MOFs can readily be synthesised that are both chiral and porous. Efforts in this area have seen the emergence of the first homochiral crystalline porous materials through two primary routes (see also Sections 1.2.3.2 and 1.2.4.2): (1) the use of chiral ligands to bridge metal ions within network topologies that would otherwise be achiral,^[29–39] as first seen in the use of a pyridine-functionalised tartrate-based ligand to form the porous homochiral 2D layered framework POST-1, which consists of honeycomb-type Zn^{II} -based layers;^[29] and (2) the use of chiral co-ligands to direct the assembly of achiral building units into chiral framework topologies,^[40–43] as first seen in the homochiral synthesis of an interpenetrated (10,3)-a network phase.^[42]

In exploiting the favourable thermodynamics and kinetics of MOF crystal growth, very large pores of uniform dimension and surface chemistry are commonly achieved that would be inaccessible by other chemical routes.^[44, 45] For example, whereas the synthesis of mesoporous silicates (*i.e.* those with pore dimensions in the range 20–500 Å) generally requires surfactant templation and calcination to leave behind amorphous hosts with regular mesopores,^[46] crystalline MOFs with pores up to 47 Å in dimension^[47] have been synthesised by the assembly of molecular building units from solution. In addition to favouring the formation of complex mesoscale architectures, the strength and directionality of the coordination bond also imparts a relatively high degree of stability to these. This is seen, for example, in their reasonably high thermal (up to ~500 °C in some cases) and chemical stabilities (albeit with susceptibility to strongly coordinating guests such as water being common), extremely low solubilities, and robustness to guest desorption (see Section 1.2.1.2). Achievement of the latter feature, which is most common in higher dimensionality (*i.e.* 2D and 3D) framework systems, has led to this field providing the most porous crystalline compounds known, with void volumes occupying as much as ~90 % of the crystal volume. The achievement of such low volumetric atom densities through the use of moderately light elements means that the gravimetric measures of porosity and surface area are also extremely high. Among a number of notable families of highly porous MOFs are members of the MOF/IRMOF family (see Figure 1.2),^[22, 48–51] MIL-*nnn* (in particular *nnn* = 100, 101),^[52, 53] ZIF-*nnn* (in particular *nnn* = 95, 100)^[54, 55] and NOTT-*nnn* series (in particular *nnn* = 100–109),^[56, 57] which provide some of the most extreme measures of porosity and surface area yet achieved: *e.g.* among these ZIF-100 (see Section 1.2.3.1.1 and Figure 1.12) and MIL-101 have the largest pores, of dimension 35.6 and 34 Å, respectively; and MOF-177 and MIL-101 have Langmuir surface areas of 5640^[58] and

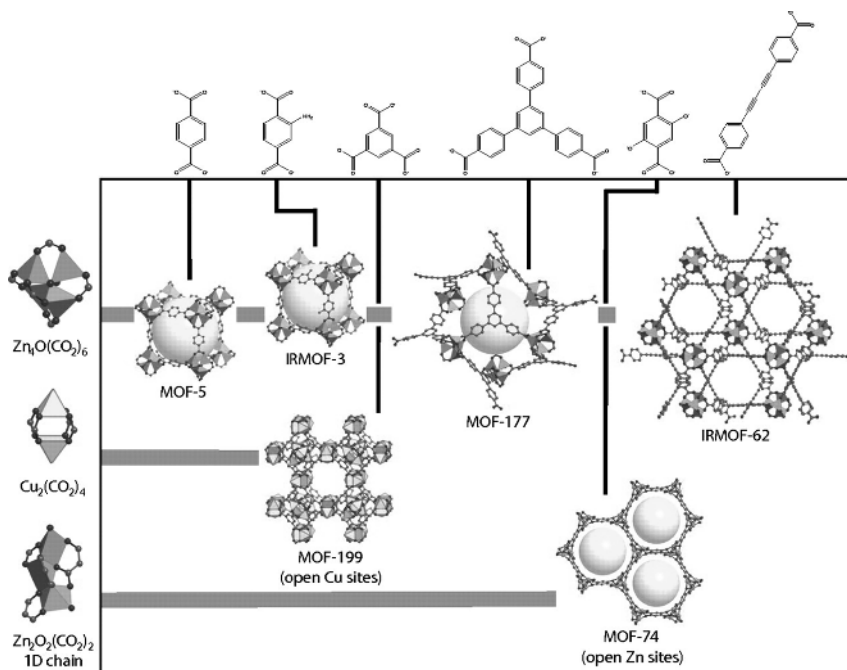


Figure 1.2 A selection of MOFs based on tetranuclear $Zn_4O(CO_2)_6$, dinuclear $Cu_2(CO_2)_4$ and 1D $Zn_2O_2(CO_2)_2$ secondary building units (left) and a range of multitopic carboxylate ligands (top). Reprinted with permission from D. Britt, D. Tranchemontagne and O.M. Yaghi, *Proc. Natl. Acad. Sci. U.S.A.*, 105, 11623. Copyright (2008) National Academy of Sciences

$5500\text{ m}^2\text{ g}^{-1}$,^[53] each more than double that of porous carbon, and gravimetric pore volumes of 1.69 ^[58] and $1.9\text{ cm}^3\text{ g}^{-1}$,^[53] respectively.

A further distinguishing feature of MOFs over other classes of porous materials is the extreme diversity of their surface chemistry, which can range from aromatic to highly ionic depending on the chemical nature of the building units used. This notably includes the achievement of multiple pore environments within individual materials.^[31] An important consequence of this versatility is that the surface chemistry can be tuned for highly specific molecular recognition and catalytic processes (see Sections 1.2.2, 1.2.3 and 1.2.4).

1.2.1.1.3 Post-Synthetic Modification of MOFs

In addition to the high degree of control over framework structure that can be achieved prior to and during MOF synthesis, considerable control can be exercised following framework assembly by exploiting the porosity of MOFs.^[1] Developments here have seen the emergence of a range of

post-synthetic approaches in which framework structure and pore chemistry are modified *via* low energy chemical pathways that involve the internal migration of guest species. These processes occur topotactically, *i.e.* with some retention of the parent structure, to generate metastable phases that are commonly inaccessible through ‘one-pot’ syntheses.^[59]

The simplest and most common form of post-synthetic modification is the desorption of guest molecules. This process, which in some cases is achieved most optimally at low temperature in multiple low-energy steps (*e.g.* through activation by volatile solvents^[60] or supercritical CO₂^[61]), commonly leads to apohost phases that are structurally stable despite having very high surface energies. This is particularly so in cases where guest desorption leaves behind bare metal sites (see Sections 1.2.2 and 1.2.4), an example being the desorption of bound water molecules from the Cu₂(CO₂)₄(H₂O)₂ ‘paddlewheel’ nodes within [Cu₃(btc)₂(H₂O)₃] (HKUST-1,^[62] also MOF-199; btc = 1,3,5-benzenetricarboxylate) (see Figure 1.3). Guest desorption influences the host–guest properties of the framework in two ways. First, in generating a large unbound surface it allows the subsequent adsorption and surface interaction of guest molecules that would not otherwise have displaced those present at the surface following MOF synthesis (*e.g.* gases, aromatics into polar frameworks). Secondly, the modification of pore contents can have a pronounced influence on framework and pore geometry, thereby greatly modifying the adsorption properties of the host (see Sections 1.2.1.2 and 1.2.3.1.2).

The exchange of guest species can also dramatically influence host framework properties. This is particularly the case for the exchange of ions within charged frameworks – a process that can change both the

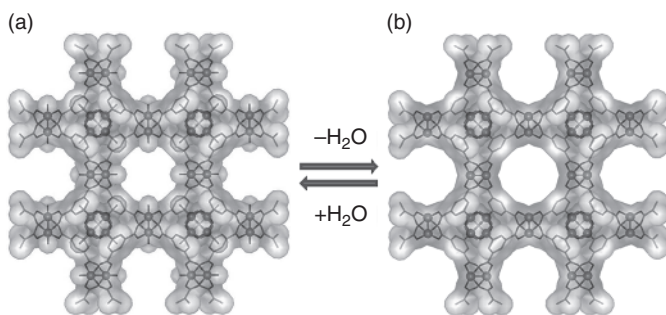


Figure 1.3 Reversible desorption of bound water molecules from the Cu₂(CO₂)₄(H₂O)₂ nodes within [Cu₃(btc)₂(H₂O)₃] (a) to produce [Cu₃(btc)₂] (b). This process occurs following the desorption of unbound guests (not shown). Cu atoms are drawn as spheres and a transparent van der Waals surface is shown

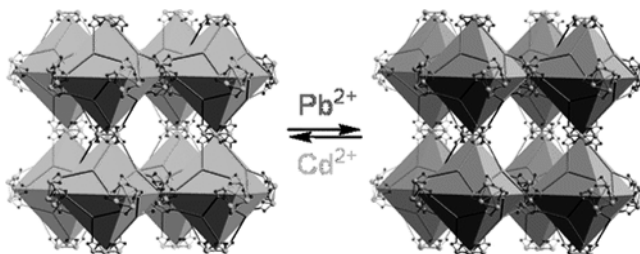


Figure 1.4 Reversible exchange of framework metal ions within $\text{Cd}_{1.5}(\text{H}_3\text{O})_3[(\text{Cd}_4\text{O})_3(\text{hett})_8]$ via a single-crystal-to-single-crystal process. Reprinted with permission from S. Das, H. Kim and K. Kim, *J. Am. Chem. Soc.*, 131, 3814. Copyright (2009) American Chemical Society

relative polarity of the framework surface and the framework geometry. In contrast to zeolites, which in consisting of anionic frameworks generally only display cation exchange, MOFs can undergo both cation^[63–65] and anion^[1, 66, 67] exchange depending on their framework charges. Whilst such processes commonly involve the exchange of labile ions within the pores, the former notably also includes the reversible exchange of metal nodes from within the framework itself, as has been seen with the replacement of Cd^{II} within $\text{Cd}_{1.5}(\text{H}_3\text{O})_3[(\text{Cd}_4\text{O})_3(\text{hett})_8]$ (where hett is an ethyl-substituted truxene tricarboxylate) by Pb^{II} (see Figure 1.4),^[68] in contrast to the analogous dealumination process in zeolites, which requires multiple steps under extreme thermal and chemical conditions, this exchange process occurs at ambient temperature. Notably, the development of ion-exchange capabilities in MOFs has numerous other points of significance, for example in the development of proton conducting frameworks.^[69, 70]

The incorporation of metal sites and other charged species into the pores of MOFs is in many cases driven by the energetics of complexation at the framework surface. Such a process may occur either through cation/anion exchange or salt inclusion. The former has been achieved, for example, with the exchange of protons with titanium(IV) di-isopropoxide at chiral BINOL units (BINOL = 1,1'-di-2-naphthol) to generate materials that display enantioselective catalytic activity.^[35, 71] The latter may involve either the complexation of metal ions at binding sites on the framework surface with concomitant inclusion of charge-balancing anions, or cation/anion complexation at bare surface metal sites with concomitant inclusion of metal complex anions/cations into the pores.^[72] The complexation of neutral metal species has also been used to modify pore chemistry, as seen with the reaction of MOF-5 with $\text{Cr}(\text{CO})_6$ to form $[\text{Zn}_4\text{O}((\eta_6\text{-}1,4\text{-benzenedicarboxylate})\text{Cr}(\text{CO})_3)_3]$, in which the aromatic

linkers now take the form of the organometallic Cr(benzene)(CO)₃ piano-stool complex.^[73]

A further strategy for framework modification involves electron transfer between host and guest, a process that in principle provides amongst the strongest of enthalpic driving forces for the inclusion (or removal) of cations or anions and for the modification of framework properties. Redox activity at both the metal and ligand sites within the framework has been achieved. An example of the former is the oxidation of [Ni^{II}₆(C₂₆H₅₂N₁₀)₃(btc)₄]*n*(-guest) (BOF-1; btc = 1,3,5-benzenetricarboxylate) by I₂, in which oxidation of some of the Ni^{II} sites to Ni^{III} results in the inclusion of triiodide ions into the pores.^[74] Examples of the latter include a number of dicarboxylate framework systems in which post-synthetic framework reduction leads to the inclusion of alkali metal ions and to dramatic changes in hydrogen gas adsorption properties of the modified framework.^[75, 76]

An equally powerful although less studied form of post-synthetic modification treats MOF crystals as chemical substrates at which covalent grafting can occur. The first use of this approach was the alkylation of unbound pyridyl units within the homochiral framework POST-1 (described in Section 1.2.1.1.2), a process that deactivates these sites catalytically.^[29] More recently, this approach has been used to confer a range of desirable host-guest properties to MOFs, with particular success seen with the grafting of a range of functional groups to the unbound amine group on the NH₂-bdc (bdc = 1,4-benzenedicarboxylate) linker within IRMOF-3.^[59] A notable consequence of this process is the modification of chemical surface properties and the fine tuning of the dimensions of the pores and pore windows, with the systematic increase in organic chain length leading to a corresponding decrease in surface area of the framework due to pore occlusion.^[77] Another notable example is the two-step attachment of a catalytically active vanadium complex through ligand grafting (with ~13 % conversion of the amine groups) followed by metal complexation to yield a material that exhibits heterogeneous catalytic activity at the vanadium centres (see Figure 1.5).^[78]

1.2.1.2 Structural Response to Guest Exchange

A common synthetic goal in MOF synthesis is the generation of frameworks that display zeolite-like rigidity to guest desorption and exchange^[31, 50, 51, 79-90] (so-called ‘2nd generation materials’) rather than collapse irreversibly upon guest removal (‘1st generation materials’).^[5] The host-guest chemistry of such systems is readily interpretable

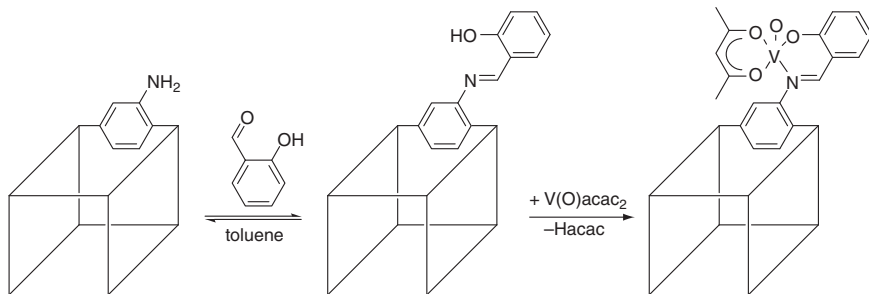


Figure 1.5 Schematic for the functionalisation of IRMOF-3 (see Figure 1.2) with salicylaldehyde and subsequent binding of a vanadyl complex (acac = acetylacetonate). Reprinted with permission from M.J. Ingleson, J.P. Barrio, J.B. Guilbaud, Y.Z. Khimyak and M.J. Rosseinsky, *Chem. Commun.*, 28, 2680–2682. Copyright (2008) Royal Society of Chemistry

using standard models, with rapid guest transport commonly occurring within the pores and Type I adsorption isotherms displayed. Importantly, these features lead to a high degree of predictability in the host–guest chemistry, with the framework structure able to be simulated as a rigid host within which dynamic guest molecules migrate and bind,^[91, 92] and with guest selectivity depending principally on the size and shape of the guest molecules and the strength of the host–guest surface interactions. Such properties are highly desirable for a wide range of host–guest applications.

In addition to the considerable interest in rigid frameworks, a very interesting feature of many MOFs is their high degree of framework flexibility. Materials of this type, which have been classified as ‘3rd generation materials’,^[5] display flexing of their framework lattices in response to various stimuli; this most commonly involves response to the desorption and exchange of guest molecules, but may also arise due to changes in temperature, pressure, irradiation, *etc.* The adsorption isotherms of materials that display guest-induced flexing typically exhibit hysteretic behaviour due to the fact that the apohost phase has a different pore structure from that of the adsorbed phase, with transformation between the two being an activated process. Structurally, the adsorption properties can range from intercalative behaviours in which staged adsorption occurs through the gradual guest-induced opening of pores (*cf.* clays) to more cooperative behaviours in which guest adsorption influences the structure of the entire MOF crystal (*i.e.* crystal and pore homogeneity are retained throughout the adsorption process). In materials of this general type the guest-selectivity is considerably more complex than that of the zeolitic phases, with adsorption commonly depending on

the strength of the host–guest interaction (which needs to be sufficient to drive the framework deformation), as well as guest size and shape considerations. This is particularly the case for mixtures of guests, where cooperative effects are commonly seen; *e.g.* the adsorption of one guest can have a ‘gate-opening’ function to allow the inclusion of a second guest that would not otherwise be adsorbed. Despite being generally less predictable than rigid frameworks, such materials have potential use in a range of applications that make use of their chemically selective adsorption and/or hysteretic behaviour (*e.g.* for guest storage). A further point of interest here is that structural modification upon guest loading provides a mechanism for molecular sensing.

At the present time it is not straightforward in all cases to predict in advance whether MOFs will survive guest desorption, or the extent to which their frameworks might distort upon desorption and subsequent adsorption. Some clear guiding principles exist, however. First, the rigidity of the building units has a clear influence on framework flexibility, with the strength of coordination bonding providing a useful initial guide as to the energetics of bond bending as well as thermal stability. Secondly, the extent of connectivity and topological underconstraint within the framework lattice has a key influence over whether low energy deformations might occur; *e.g. cf.* rigidity of triangular network *vs* scissor action of square grid. In considering whether host–guest interaction energies are sufficient to drive framework deformation or decomposition, a particularly important consideration is whether guests may bind at the metal nodes and thereby favour pronounced structural flexing, framework interconversion or even dissolution; a relatively common limitation of MOFs is their sensitivity to water vapour, with the metal nodes in some systems being susceptible to water binding and ligand displacement. More subtle effects such as hydrogen bonding interactions, or even weak intermolecular forces involving small gaseous guests, can frequently be sufficient to cause pronounced framework flexing.

1.2.1.2.1 Flexible Frameworks

Two different types of guest-induced flexibilities exist in MOF host lattices. The first can be considered as essentially static in nature, involving bulk framework deformations that may be readily characterised using diffraction-based techniques and which are frequently observable at the macroscale through changes in crystal dimensions. The second are dynamic and arise due to molecular vibrations or local guest-induced framework deformations away from the ‘parent’ structure. The latter are not so readily detectable by diffraction methods and

are commonly inferred based on geometric considerations; for example, local distortions away from the bulk crystallographic structure have been shown to be necessary in certain cases to allow migration of guests through narrow pore windows.^[93] Given these complexities, considerations of the guest selectivity of flexible systems need necessarily extend beyond simple ‘size and shape’ arguments towards the more complex consideration of guest-driven host lattice modification.

A broad array of interesting flexing behaviours have been seen in MOF systems, spanning intercalative-type behaviour in 2D layered systems to the deformation of individual frameworks and the translation of interpenetrated frameworks.^[74, 79, 85, 94–99] The interdigitated 2D layer compound $[\text{Cu}(\text{dhbc})_2(4,4'\text{-bpy})] \cdot n(\text{guest})$ (dhbc = dihydroxybenzoate; 4,4'-bpy = 4,4'-bipyridine) displays pronounced interlayer contraction upon guest desorption, with a 30 % decrease in the *c*-axis length.^[100] This process occurs without loss of polycrystallinity and involves the gliding of aromatic units with respect to each other. Subsequent adsorption of guest molecules leads to regeneration of the more open structure, with the corresponding adsorption isotherms displaying activated, hysteretic behaviour in which a ‘gate-opening’ pressure is required before adsorption can occur.

The interdigitated bilayer phase $[\text{M}^{\text{II}}_2(4,4'\text{-bpy})_3(\text{NO}_3)_4] \cdot n(\text{guest})$ (*M* = Ni, Co, Zn)^[79, 89, 93, 101] displays zeolite-like robustness upon desorption of ethanol guests from the parent phase^[82] and two types of framework flexibility upon adsorption of other guests.^[79] *In situ* single crystal diffraction characterisation during guest adsorption showed that molecular guests with dimensions too large for the pores of the apohost can be adsorbed due to a progressive widening of the 1D pores with increasing guest size associated with low energy scissor-type flexing of the bilayers. Even larger guests are adsorbed into this phase through a different pore expansion mechanism in which translation of the interpenetrated bilayer nets with respect to each other leads to an increase in the height of the 1D channels.

The MIL-53 family of 3D frameworks, with formula $[\text{M}^{\text{III}}(\text{OH},\text{F})(\text{bdc})] \cdot n(\text{guest})$ (*M* = Al, Cr, Fe; bdc = 1,4-benzenedicarboxylate), also display scissor-type flexing as a function of temperature and guest adsorption with considerable variation in the dimensions of the 1D channels.^[102, 103] A comprehensive *in situ* powder X-ray diffraction examination of guest adsorption into the Fe analogue, MIL-53(Fe), has demonstrated that the guest-induced breathing effect depends principally on the strength of the interaction between host and guest rather than being particularly dependent on guest size (see Figure 1.6).^[102] The principal

temperature and light irradiation) leads to a modification of framework connectivity. These may be classified into cases in which structural interconversion requires the breakage and formation of coordination bonds, and those where changes to the covalent connectivity arises.

Coordinative interconversion Whilst the majority of porous MOFs retain their structural connectivity during guest-exchange processes, in an increasing number of systems the dynamic nature of the metal-ligand bond in solution has been mirrored in the solid state, yielding highly pronounced structural interconversions. Lability at the metal nodes in these systems can arise due either to a dissociative or associative mechanism, with each of these being influenced by neighbouring coordinating guests within the pores and/or by unbound donor sites on the framework ligands. Confirmation that the structural interconversions are topotactic processes within the solid state rather than solvent-assisted recrystallisations has been provided by *in situ* diffraction measurements in which the interconversions are followed in real time. This coordinatively dynamic nature of some MOF lattices is evidenced also by the demonstration that MOF synthesis can be achieved under essentially solvent free conditions at ambient temperature following initiation of the solid state reaction by ball milling,^[105] and by the single-crystal-to-single-crystal exchange of metal nodes by immersion of MOF crystals in the solution of other metal ions.^[68]

The simplest and most common form of framework interconversion involves disassociation of terminal ligands followed by intra-/interframework complexation. In $[\text{Fe}^{\text{II}}(\text{pmd})(\text{H}_2\text{O})(\text{M}^{\text{I}}(\text{CN})_2)_2]\cdot\text{H}_2\text{O}$ (pmd = pyrimidine; $\text{M}^{\text{I}} = \text{Ag}, \text{Au}$), for example, thermal desorption of the bound water molecules leads to the coordination of a pmd ligand from an interpenetrated network, thereby linking the networks together.^[106] This results in a topochemical conversion in which there is a change in the framework topology from the interpenetration of three separate 3D networks to a single 3D network. Interesting changes to the spin-switching properties result from this transformation (see Section 1.3.2.1). Another form of thermally induced structural interconversion is seen in $[\text{Cu}(\text{CF}_3\text{COCHCOC}(\text{OCH}_3)(\text{CH}_3)_2)_2]$, for which temperature pulsing causes a conversion from a porous phase containing exclusively the *trans*-isomer of the Cu^{II} complex to a dense phase containing a mixture of *cis*- and *trans*-isomers.^[107] Subsequent exposure of the dense phase to adsorptive vapour reverts the material to its porous form.

Exposure to solvent vapour can also drive pronounced framework interconversion in which coordination bond breakage and formation occurs.^[41, 42, 93, 108] An example here is a family of frameworks

incorporating the 1,3,5-benzenetricarboxylate (btc) linker, for which exchange of bound solvent at the metal nodes is accompanied by structural conversions between a range of different network topologies.^[41, 42] Guest desorption from the homochiral framework $[\text{Ni}_3(\text{btc})_2(\text{py})_6(1,2\text{-pd})_3] \cdot n(\text{guest})$ (btc = 1,3,5-benzenetricarboxylate; py = pyridine; 1,2-pd = 1,2-propanediol), which consists of the interpenetration of two (10,3)-a networks, leads to an amorphous phase in which the long-range structural order is lost. Subsequent exposure to ethanol vapour leads to the regeneration of the ordered double-network structure, which upon prolonged exposure converts to a more dense quadruply interpenetrated (10,3)-a network phase (see Figure 1.7).^[43] The latter is the same phase as crystallises from ethanolic solution, indicating that ethanol adsorption into the doubly interpenetrated network leads to a metastable topotactic phase that gradually converts to a more stable phase over time. In contrast, exposure to pyridine leads to the formation of a 2D hexagonal sheet structure, also requiring breakage and formation of coordination bonds, whereas 3-picoline adsorption leads to stabilisation of the doubly interpenetrated phase above that of the parent material; this phase is homochiral with 47 % permanent porosity and displays enantioselective guest-exchange.^[41]

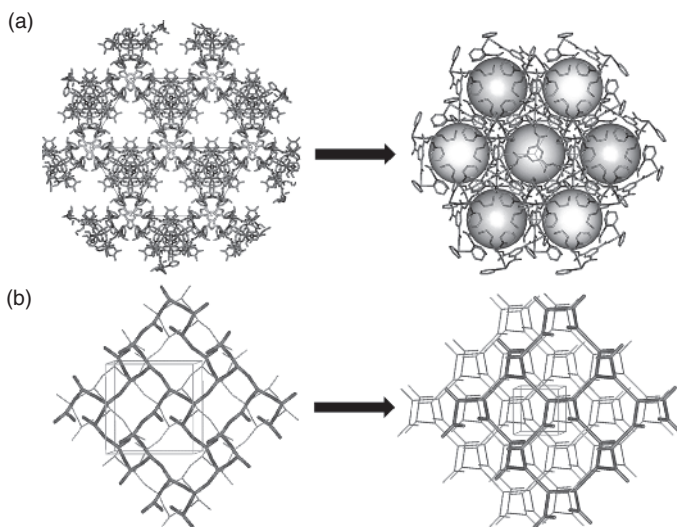


Figure 1.7 Interconversion of the highly porous, homochiral 3D MOF $[\text{Ni}_3(\text{btc})_2(\text{py})_6(1,2\text{-pd})_3] \cdot n(\text{guest})$ upon guest desorption and exposure to ethanol vapour (a), involving transformation from a doubly interpenetrated, distorted (10,3)-a network phase to one in which four regular (10,3)-a nets interpenetrate (b). Reprinted with permission from C.J. Kepert, T.J. Prior and M.J. Rosseinsky, *J. Am. Chem. Soc.*, **122**, 5158. Copyright (2000) American Chemical Society

Covalent interconversion The modification of MOF structure through topochemical reactions between organic linkers rather than through coordinative exchange is comparatively rare due to the less labile nature of covalent bonds. Some noteworthy examples exist, however, in which the organic units are favourably aligned within the framework to react with each other if induced to do so thermally or by photoexcitation. A particular point of interest here is the stereoselectivity of this process, with the regularity of the framework structure often imparting isomeric purity in the covalent product.^[109]

A highly strategic example of this approach is seen in the [2 + 2] cycloaddition of adjacent *trans*-1,2-bis(4-pyridyl)ethene (tvp) linkers within a number of 1D ladder-type frameworks in which dinuclear metal complex 'rungs' align the tvp molecules side-to-side.^[110–112] In the ladder framework $[(\text{CF}_3\text{CO}_2)(\mu\text{-O}_2\text{CCH}_3/\text{Zn})_2(\mu\text{-tvp})_2]$ this dimerisation process occurs *via* a single-crystal-to-single-crystal transformation, allowing detailed structural characterisation of the product (see Figure 1.8).^[112] Ligand polymerisation can also occur, as seen for example with the irradiation of $[\text{Ca}(\text{C}_4\text{H}_5\text{O}_2)_2(\text{H}_2\text{O})]$ with ^{60}Co γ -rays to yield high molecular weight calcium poly(3-butenolate) (average $400\,000\text{ g mol}^{-1}$) in 97 % yield.^[113] While not a form of framework conversion it warrants mention here that the polymerisation of adsorbed organic guests within MOFs has also been achieved with a high degree of stereoselectivity.^[114]

1.2.2 Storage and Release

The very large pores and high surface areas of MOFs, combined with their potential low cost, low toxicities and industrial scalability, makes them outstanding candidates for the storage and release of a range of different guest molecules.^[115] In the development of guest storage technologies, considerable current focus is on industrially important gases

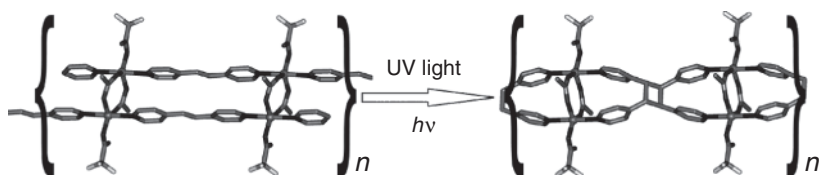


Figure 1.8 Structural conversion of a 1D ladder framework induced by photochemical excitation. Reprinted with permission from N.L. Toh, M. Nagarathinam and J.J. Vittal, *Angew. Chem. Int. Ed.*, **44**, 2237. Copyright (2005) WILEY-VCH Verlag GmbH & Co. KGaA

such as hydrogen,^[116–119] methane^[51, 88, 120] and acetylene,^[121, 122] and extends also to the controlled release of larger guests such as pharmaceuticals.^[123–125] Given that each of these areas is currently undergoing very rapid advance, a brief description is given here to the development of hydrogen storage materials, for which reasonably detailed structural–property relationships have emerged.

1.2.2.1 Hydrogen Storage

The efficient storage of hydrogen gas is a critical challenge that needs to be met if hydrogen-based energy cycles are to displace those based on fossil fuels. The US Department of Energy 2010 targets for vehicular hydrogen storage systems are a capacity of 6 wt% H₂, 45 g H₂ L⁻¹, an ability to operate in the temperature range –30 to 50 °C to a maximum pressure of 100 bar, reversibility over 1000 cycles, and a refuelling rate of at least 1.5 kg H₂ min⁻¹; the 2015 targets stipulate a *ca* 50 % improvement to these numbers. Among a wide range of physisorption phases (*i.e.* those where dihydrogen interacts with the surface through an intermolecular interaction), MOFs have shown the highest H₂ uptakes, being greater than those for porous carbons and zeolites and exceeding both the gravimetric and volumetric targets for hydrogen adsorption.^[116–119] In comparing the potential of MOFs with that of chemisorption phases (*i.e.* those where hydrogen reacts to form a covalent or ionic compound; *e.g.* metal hydrides) a number of advantages exist relating to the much lower enthalpy of adsorption/desorption, resulting in much reduced heat flow requirements during refilling and to the highly reversible nature of the process, both for hydrogen and various contaminants.

Among a large number of different MOFs investigated for their hydrogen storage capabilities, the IRMOF (isoreticular metal-organic framework) series with formula [Zn₄OL₃] (where L = a range of dicarboxylates)^[60, 126, 127] and NOTT-10*n* (*n* = 1–7) series with formula [Cu₂L] (where L = a range of tetracarboxylates)^[56, 57] display adsorption properties that are both impressive and highly informative. A notable trend to emerge from the study of these and related systems is a reasonably strong correlation between hydrogen adsorption and BET and Langmuir N₂ surface area (see Figure 1.9), a relationship that provides a useful predictive tool for surface saturation loading of H₂.^[117] Of these materials, the highest excess uptake (*i.e.* the uptake beyond that which would be contained within a free volume equivalent to that of the sample) is seen in MOF-5, which adsorbs 7.1 wt% at 77 K and 40 bar, with a

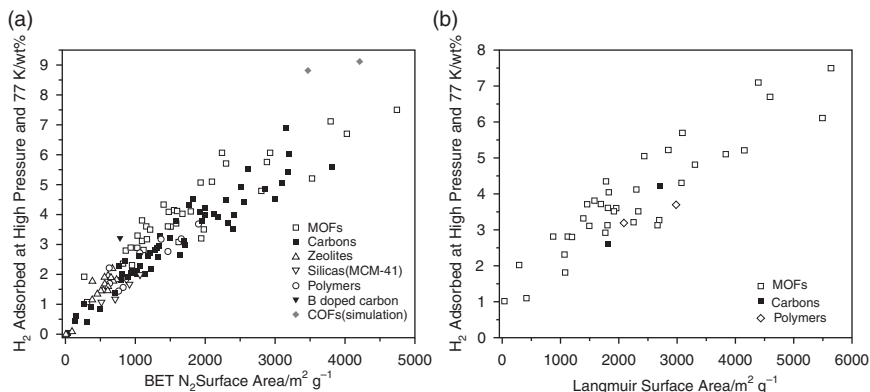


Figure 1.9 The variation of H₂ adsorbed (wt%) at saturation at 77 K with BET (a) and Langmuir surface area (b) for porous MOFs, carbons, zeolites, silicas, polymers, and covalent organic frameworks (COFs). Reprinted with permission from K.M. Thomas, *Dalton Trans.*, **9**, 1487–1505. Copyright (2009) Royal Society of Chemistry

total uptake of 10.0 wt% at 100 bar and a volumetric storage density of 66 g l⁻¹.^[127] The larger pore material MOF-177, [Zn₄O(BTB)₂] (where BTB = 1,3,5-benzenetricarboxate), achieves an excess uptake of 7.1 wt% at 77 K and 66 bar, but with a lower volumetric density of 49 g l⁻¹ on account of its lower surface density.^[128] A comparable volumetric uptake is seen in NOTT-103.^[56]

Whilst a number of important benefits exist for the physisorption approach to hydrogen storage over that of chemisorption materials, the weakness of the hydrogen-surface interaction, which is typically in the order of 4–6 kJ mol⁻¹, represents a considerable technological limitation. For such interaction enthalpies surface saturation can only be achieved at low temperatures or prohibitively high pressures; as a representative example, the hydrogen capacity of MOF-5 drops to 0.57 wt% and 9.1 g l⁻¹ at 298 K and 100 bar.^[127] Theoretical calculations indicate that enthalpies of *ca* 20 kJ mol⁻¹ are required for optimal performance at ambient temperature with pressures up to 30 bar.^[116] Recent efforts to develop hydrogen storage capabilities at ambient conditions have focused on the generation of highly charged framework surfaces, in particular those having bare metal sites where dihydrogen can interact directly;^[65, 75, 76, 129–132] notably, this approach has also proven useful for the optimal storage of methane^[120] and acetylene.^[122] Currently, the maximum isosteric enthalpies of adsorption in MOFs are ~12–13 kJ mol⁻¹, achieved through dihydrogen binding at bare Ni^{II} and Cu^{II} sites.^[133, 134] The highest ambient temperature hydrogen uptake is seen, however, in Mn₃[(Mn₄Cl)₃(BTT)₈]₂ (where

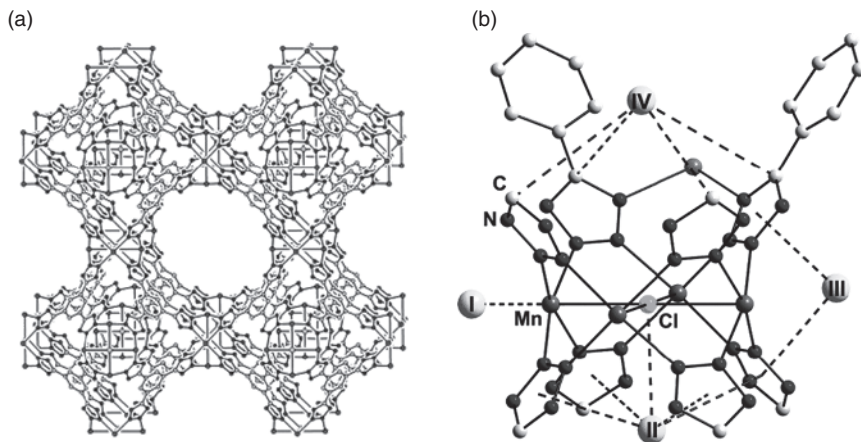


Figure 1.10 (a) The anionic framework structure of $[\text{Mn}(\text{DMF})_6]_3[(\text{Mn}_4\text{Cl})_3(\text{BTT})_8(\text{H}_2\text{O})_{12}]_{2-n}(\text{guest})$ shown with $[\text{Mn}(\text{DMF})_6]^{2+}$ units and guests removed. (b) Principal surface dihydrogen binding sites as determined by powder neutron diffraction. Reprinted with permission from M. Dincă, A. Dailly, Y. Liu, C.M. Brown, D.A. Neumann and J.R. Long, *J. Am. Chem. Soc.*, **128**, 16876. Copyright (2006) American Chemical Society

BTT = 1,3,5-benzenetristetrazolate), which combines a high surface area ($2100 \text{ m}^2 \text{ g}^{-1}$) with a high surface density of bare Mn^{II} sites (physisorption enthalpy = 10.1 kJ mol^{-1} at zero loading) to adsorb 12.1 g l^{-1} (7.9 g l^{-1} excess) of hydrogen at 90 bar and 298 K (see Figure 1.10);^[129] this is 77 % greater than the density of compressed hydrogen gas under these conditions.

A further potentially beneficial feature of MOFs is their hysteretic adsorption behaviour, which in principle can be exploited to allow hydrogen loading at very high pressures/low temperatures and release at lower pressures/higher temperatures. Such a property is seen in $[\text{Ni}_2(4,4'\text{-bpy})_3(\text{NO}_3)_4]$, a framework with narrow windows that displays scissor-type flexibility upon adsorption and desorption of guests (see Section 1.2.1.2.1); adsorption isobars reveal that H_2 desorption commences only upon warming above $\sim 110 \text{ K}$, a property that is attributed to the kinetic trapping of dihydrogen in this phase.^[135]

1.2.3 Selective Guest Adsorption and Separation

Many of the properties that make MOFs excellent candidates for molecular storage, such as their very high surface areas, adjustable pore sizes and tunable surface properties, also make them particularly well suited for application in the separation of molecular and ionic mixtures. Of

particular technological interest here is the development of materials that are able to perform highly selective separations efficiently, rapidly, and on the bulk scale. Strategically important species range from gases (*e.g.* H₂, He, O₂, N₂, CO, CO₂, CH₄ and other alkanes, H₂S, NO_x, NH₃, *etc.*), as present in air, flue gases, natural gas, syn-gas, *etc.*)^[136] to ions (*e.g.* [NO₃]⁻, [SO₄]²⁻, [TcO₄]⁻, Cs⁺, Sr²⁺, *etc.*)^[137] to large molecules such as pharmaceuticals and their precursors (many requiring enantioseparation).^[138, 139] Large-scale target technologies for the former include H₂ and CH₄ purifications, CO₂ capture, CO removal for fuel cell technology, and desulfurisation of transportation fuels.

Adsorptive separations by porous materials are commonly achieved by one or more of the following mechanisms: (1) size/shape exclusion; (2) selective adsorbate–surface interactions; (3) different guest diffusion rates; and (4) the quantum sieving effect, in which small guests are adsorbed faster than larger ones due to their more rapid diffusion through narrow pore windows. Manipulation of these effects requires control over both pore structure and surface chemistry, each of which may be achieved strategically to a high level of sophistication in the synthesis and post-synthetic modification of MOFs. Moreover, in contrast to more conventional porous materials such as zeolites, the structural flexibility of many MOFs gives them a vastly more complex behaviour in which selectivity may depend, uniquely, on the ability of the guest molecule to distort the host framework.

1.2.3.1 Gas Adsorption

Considerable recent efforts have been devoted to the investigation of gas separation in both rigid and porous MOF phases. Whilst only a relatively small number of systems have been investigated by selective gas adsorption measurement (as opposed to multiple measurement with various pure gases, which due to cooperative effects provides only a guide to the separation capabilities), a number of distinct separation mechanisms have been evidenced.^[136]

1.2.3.1.1 Rigid MOFs

Gas separation based on size/shape exclusion has been achieved in a relatively large number of small pore frameworks. The 3D diamond-type framework [Mn^{II}₃(HCOO)₆], for example, selectively adsorbs H₂ over N₂ and Ar at 78 K and CO₂ over CH₄ at 195 K. Uptakes of the excluded gases N₂, Ar and CH₄ are almost zero due to their inability

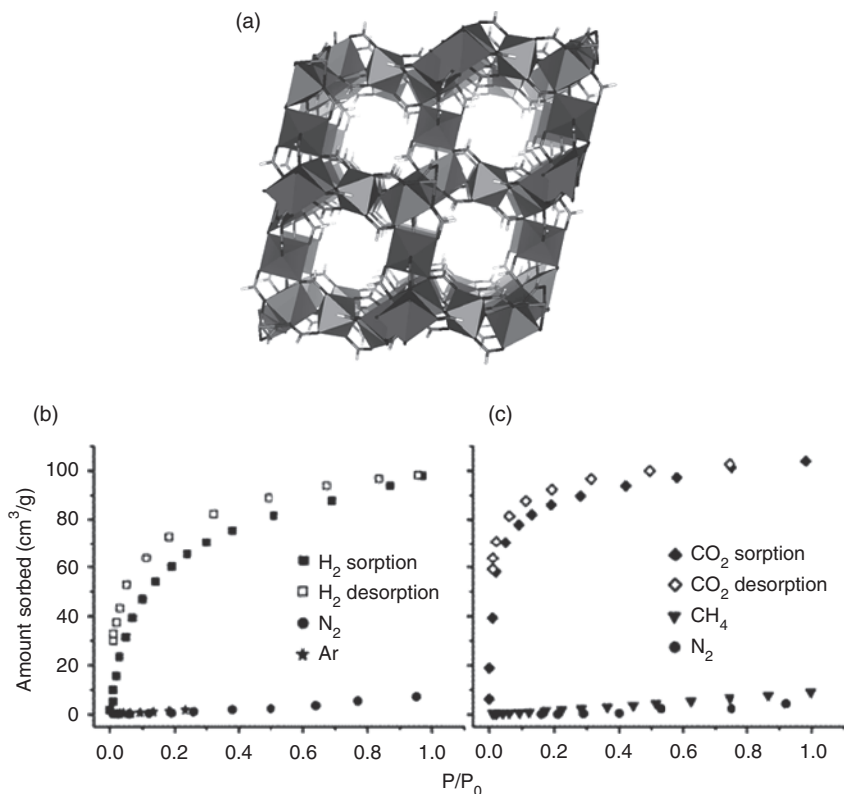


Figure 1.11 Structure of $[\text{Mn}^{\text{II}}_3(\text{HCOO})_6]$ (a) and gas adsorption isotherms at 78 K (b) and 195 K (c). Reprinted with permission from D.N. Dybtsev, H. Chun, S.H. Yoon, D. Kim and K. Kim, *J. Am. Chem. Soc.*, **126**, 32. Copyright (2004) American Chemical Society.

to migrate through the very narrow pore windows of this phase (see Figure 1.11).^[140] The size-selective separation of N₂ and O₂, which have extremely similar molecular dimensions and are separated industrially by ion-exchanged zeolites (*e.g.* CaX/NaX) according largely to the difference in their quadrupolar moments, has reportedly been achieved by $[\text{Mg}_3(\text{ndc})_3]$ (ndc = naphthalenedicarboxylate),^[141] $[\text{Zn}(\text{dtp})]$ (dtp = 2,3-di-1*H*-tetrazol-5-ylpyrazine),^[142] and $[\text{Zn}_4\text{O}(\text{H}_2\text{O})_3(\text{adc})_3]$ (PCN-13; adc = 9,10-anthracenedicarboxylate).^[143]

In addition to molecular sieving effects, which make use of different diffusivities of the different guests, the fine control over MOF surface chemistry has seen the emergence of materials that discriminate gases according to the strength of their adsorption interaction. An example here is the 3D pillared layer phase $[\text{Cu}_2(\text{pzdc})_2(\text{pz})]$ (where

pzdc = pyrazine-2,3-dicarboxylate and pz = pyrazine), which selectively adsorbs acetylene over CO_2 due to the preferential docking of the former between two basic oxygen atom sites within the framework's highly constrained 1D pores (dimensions $4 \times 6 \text{ \AA}$) rather than to a size-selective molecular sieving effect.^[121] The much larger pores of zeolitic imidizolate frameworks (ZIFs) also display a high degree of chemical selectivity, with capture of CO_2 from CO_2/CO mixtures attributed to the different binding affinities of these gases.^[144] Breakthrough experiments, in which a continuous flow of 1:1 CO/CO_2 was passed through packed columns of ZIF-68, 69 and 70, further demonstrated the complete retention of CO_2 and passage of CO . In the related phases ZIF-95 and 100, which contain narrow pore windows (3.65 and 3.35 \AA , respectively) between colossal pores, a similarly high selectivity for CO_2 adsorption over other gases was attributed to a combination of molecular sieving and surface selectivity effects, the latter arising due to quadrupolar interactions of CO_2 with the nitrogen atoms on the pore surface (see Figure 1.12).^[54]

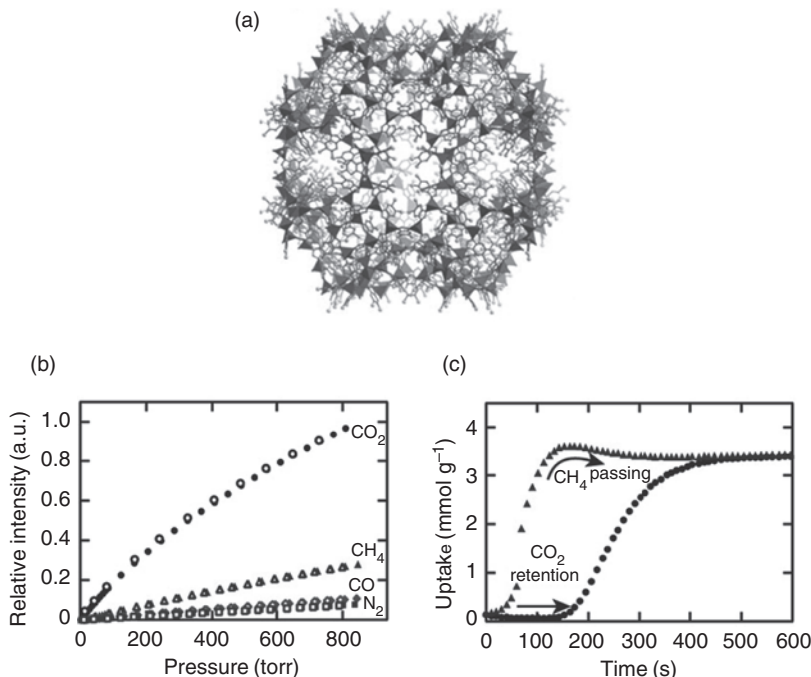


Figure 1.12 (a) The 35.6 \AA cage within ZIF-100, which is accessed through narrow pore windows. (b) CO_2 , CH_4 , CO and N_2 gas adsorption isotherms for ZIF-100 at 298 K. (c) CO_2/CH_4 breakthrough curves, showing the retention of CO_2 within a packed column. Reprinted with permission from B. Wang, A.P. Cote, H. Furukawa, M. O’Keeffe and O.M. Yaghi, *Nature*, 453, 207 (2008).

Whilst the above separations require cycling through adsorption and desorption processes, typically through swings in pressure or temperature, excellent potential exists for the achievement of continuous-flow separation through the development of MOF membranes. This has been achieved through oxidative electrodeposition of thin films of $[\text{Cu}_3(\text{btc})_2]$ (HKUST-1) at a Cu metal mesh.^[145] These membranes display permeabilities and selectivities that are superior to those of conventional zeolite membranes, with the high H_2 permeation flux ($0.107 \text{ mol m}^{-2} \text{ s}^{-1}$) leading to ambient temperature separation factors of 7.04, 6.84, and 5.92 from 1:1 mixtures of H_2/N_2 , H_2/CO_2 , and H_2/CH_4 , respectively. The recyclability and high chemical and thermal stability of these membranes makes them strong candidates for bulk-scale hydrogen separation and purification.

1.2.3.1.2 Flexible MOFs

Selective gas adsorption and separation in flexible MOFs is considerably more complicated than that in their rigid counterparts. Due to the high degree of cooperativity in these systems (*e.g.* in inducing framework deformation, the uptake of one guest can dramatically alter the uptake of another), comparison of adsorption isotherms of pure gases is of limited use and competitive measurements are essential if separation capabilities are to be determined. Due to the fact that such measurements remain very rare, and that structural information is often unavailable for the mixed-sorbed phases, only limited understandings of gas separations in flexible MOFs currently exist.

The simplest form of selective adsorption in flexible MOFs involves a molecular sieving effect where, for example, small guests deform the host lattice to allow their inclusion while larger guests are excluded. This property is seen in $[\text{Cd}(\text{pzdc})(\text{bpee})]$ (where $\text{pzdc} = \text{pyrazine-2,3-dicarboxylate}$ and $\text{bpee} = \textit{trans}$ -1,2-bis(4-pyridyl)ethene, also tvp), with water and methanol adsorption occurring and inducing expansion of the 1D channels whilst larger guests such as ethanol, tetrahydrofuran and acetone are excluded under all conditions.^[146] More complicated are cases where differing degrees of pore expansion occur for different guests, as seen in materials such as $[\text{Cu}^{\text{II}}(\text{dhbc})_2(4,4'\text{-bpy})] \cdot n(\text{guest})$ (see Section 1.2.1.2.1).^[100] The separation capabilities of such phases are yet to be determined through competitive measurements and seem likely to depend principally on host-guest interaction enthalpies.

For weakly interacting guests, the exploitation of temperature rather than guest-induced gate-opening as a means to vary pore window dimensions – an effect that is seen in a number of zeolite and related materials – has led to

the development of size-selective adsorption properties in MOFs that may be varied thermally. The flexible 3D framework phase $[\text{Ni}^{\text{II}}_8(5\text{-bbdc})_6(\mu_3\text{-OH})_4]$ (MAMS-1; 5-bbdc = 5-*tert*-butyl-1,3-benzenedicarboxylate) contains narrow pore windows that range in dimension from 2.9 to 5.0 Å depending on temperature,^[147] an effect that is considerably larger than that seen in zeolites. Adsorption isotherms for a range of small gases into this phase show strong temperature dependencies; for example, no appreciable N_2 is adsorbed at 77 and 87 K whereas considerable adsorption is achieved at 113 K. These effects were attributed principally to thermally induced gate-opening rather than increased thermal excitation of the guests through the narrow hydrophilic pore windows.

1.2.3.2 Liquid Phase Adsorption

The separation of larger molecules, which requires adsorption from liquids/solutions rather than the gas phase, has also received some attention. Indeed, arguably the first demonstrations of guest selective adsorption in this field involved the separation of solvent mixtures using Hofmann-type clathrate phases of formula $[\text{M}(1)^{\text{II}}\text{L}_2\text{M}(2)^{\text{II}}(\text{CN})_4] \cdot n(\text{guest})$ (where $\text{M}(1)$ = divalent octahedral transition metal; L = unidentate ligand such as NH_3 ; $\text{M}(2)$ = Ni, Pd, Pt).^[148, 149] These materials can be used as liquid chromatographic stationary phases for the separation and purification of a range of small molecules, with high degrees of guest selectivity and moderately rapid rates of guest exchange (albeit too slow to be competitive industrially) occurring despite their 2D collapsible nature. Guest-specific docking in these phases occurs in rigid elongated pores that are bound by the $\text{M}(2)$ and L groups, with the docking of aromatics such as benzene being particularly favoured at these sites.

In targeting large-scale separation processes from the liquid phase, for which well-established technologies exist, MOFs offer arguably the greatest promise in specialist areas that make use of their unique guest selectivities. One particularly notable opportunity is in the field of enantioseparations, for which classical porous materials such as zeolites have made little impression due to the difficulty of preparing enantiomerically pure examples with free void volume; current enantioseparation technologies are based largely on nonporous surface-modified formulations that have limited chemical stability. Following the successful generation of the first homochiral porous phases (see Section 1.2.1.1.2), subsequent investigations of enantioselective guest-exchange have led to some of the first demonstrations of chiral separation using crystalline porous

materials.^[34, 42, 150] The robust 3D framework $[\text{Ni}_3(\text{btc})_2(3\text{-pic})_6(1,2\text{-pd})_3]\cdot n(\text{guest})$ (3-pic = 3-picoline), which is obtained through post-synthetic modification of the pyridine analogue (see Section 1.2.1.2.2 and Figure 1.7) and contains a helical pore structure that occupies *ca* 50 % of the crystal volume, enantioselectively adsorbs 1,1'-bi-2-naphthol with an enantiomeric excess (*ee*) value of 8.3 %. Among a diverse range of frameworks constructed using chiral BINOL-based ligands,^[35, 151–154] $[\text{Gd}(\text{R-}L\text{-H}_2)(\text{R-}L\text{-H}_3)(\text{H}_2\text{O})_4]$ (where *L* = 2,2'-diethoxy-1,1'-binaphthalene-6,6'-bisphosphonate) achieves a 13.6 % enantio-enrichment of racemic *trans*-1,2-diaminocyclohexane. The highest degrees of enantioselectivity have been seen using smaller pore frameworks, in which a more effective multi-point interaction between guest and host surface typically occurs. The 3D pillared layer framework $[\text{Ni}_2(\text{L-asp})_2(4,4'\text{-bpy})]\cdot n(\text{guests})$ (L-asp = L-aspartate), which has 23 % pore volume and pore windows of dimension $3.8 \times 4.7 \text{ \AA}$, enantioselectively adsorbs a range of racemic mixtures, with the highest *ee* value of 53.8 % achieved for the separation of racemic 2-methyl-2,4-pentanedione.^[30] Most impressively, almost complete enantioseparation of 2-butanol (*ee* = 98.2 %) is achieved with the immersion of the robust diamond-type framework $[\text{Cd}(\text{QA})_2]$ (QA = 6'-methoxyl-(8*S*,9*R*)-cinchonan-9-ol-3-carboxylate) in the racemic liquid.^[155]

Enantioselective exchange of chiral cations has also been achieved in homochiral MOF systems. The 2D framework POST-1, described in Section 1.2.1.1.2, contains 1D homochiral pores within which both enantioselective guest exchange and catalysis occurs.^[29] Upon suspension of L-POST-1 in a methanol solution of racemic $[\text{Ru}(2,2'\text{-bpy})_3]\text{Cl}_2$ (2,2'-bpy = 2,2'-bipyridine), 80 % of the exchangeable protons are exchanged with the propeller-type cation, with *ee* = 66 % in favour of the D form.

1.2.4 Heterogeneous Catalysis

1.2.4.1 Overview

Heterogeneous catalytic activity was one of the first proposed^[11] and demonstrated^[156] host-guest properties of MOFs, with subsequent research providing a range of different catalytic activities across a diverse array of framework systems.^[157, 158] Most notable among these systems are cases in which catalysis arises due to chemical activation at specific surface binding sites.

In conceptualising the catalytic capabilities of MOFs a useful first point of comparison is with zeolites, with which they share a number of common attributes: considerable pore sizes and volumes, allowing inclusion and reaction of large precursor molecules; robustness to guest desorption and adsorption, allowing rapid molecular transport; regularity of pore structure, imparting a degree of size selectivity to the catalytic process based on the shape/size of the reactant, intermediate, or product; and, in some cases, high thermal stability (up to *ca* 500 °C), albeit lower than that of most zeolites. At the other end of the spectrum, MOFs notably share many attributes with enzymes, in that sophisticated catalytic sites can, in principle, be incorporated into the framework structure to yield specific types of activity.^[159] A notable point here is that highly active surfaces can be achieved through two means: the intrinsic strain of MOF lattices, in which the high lattice binding energies in many cases favour the stabilisation of unusual molecular and coordination geometries; and through post-synthetic modification to generate metastable high energy sites not otherwise accessible through ‘one-pot’ reactions. Given this positioning, the pursuit of catalytic applications for MOFs has to date centred principally on high-end reactions (*e.g.* to produce enantiomers and fine chemicals) rather than those requiring forcing conditions.

1.2.4.2 Synthetic and Post-Synthetic Approaches

1.2.4.2.1 Metal Sites

Several different approaches have been used to incorporate active metal sites onto the interior surfaces of MOFs. Foremost among these is the often adventitious generation of reactive metal nodes by framework formation, with the first example of this type being the 2D layered structure [Cd(4,4'-bpy)₂(NO₃)₂], which catalyses the cyanosilation of aldehydes.^[156] The shape-selective activity of this system is attributable to the Lewis acidity of the labile Cd^{II} nodes and their geometric constraint within the square grid layers. The subsequent generation of framework phases that are stable to metal site activation through the desorption of bound solvent molecules has generated a number of more advanced catalytic systems.^[160–163] These include the well-known [Cu₃(btc)₂] (HKUST-1, MOF-199; btc = 1,3,5-benzenetricarboxylate) (see Figures 1.2 and 1.3),^[160, 161] and [Cr₃F(H₂O)₂O(bdc)₃] (MIL-101; bdc = 1,4-benzenedicarboxylate),^[162] each of which catalyse cyanosilylation reactions, with the latter acting as a stronger Lewis acid than the former due to the greater relative acidity of Cr^{III} over Cu^{II}.

More strategic efforts to incorporate specific metal site function into MOFs have seen the construction of lattices using dedicated metallo-ligands. An excellent example here is the use of chiral Mn-salen units to pillar square grid layers of form $Zn_2(\text{bpdc})_2$ (bpdc = biphenyldicarboxylate) (see Figure 1.13).^[164] This material functions as an enantioselective catalyst for olefin epoxidation, yielding *ee* values >80 %. Framework confinement of the manganese salen entity enhances catalyst stability, imparts substrate size selectivity, and permits catalyst separation and reuse, whilst retaining the

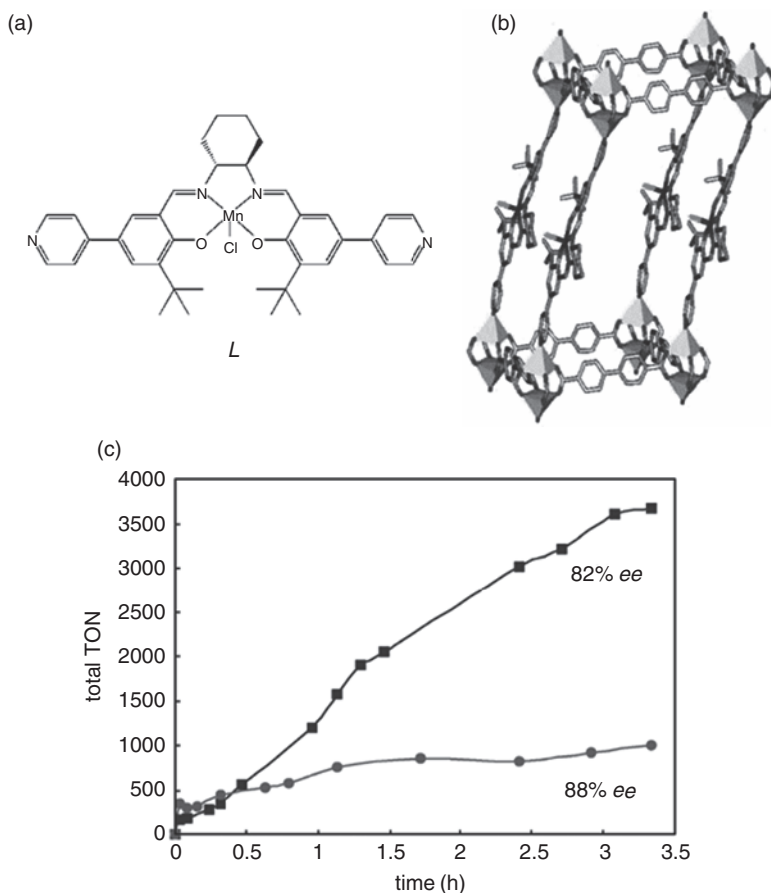


Figure 1.13 (a) Catalytically active bis-pyridyl Mn-salen metalloligand *L*. (b) Framework structure of $[Zn_2(\text{bpdc})_2L] \cdot n(\text{guest})$. (c) Plots of total turnover number (TON) vs time for the enantioselective epoxidation of 2,2-dimethyl-2H-chromene catalysed by $[Zn_2(\text{bpdc})_2L] \cdot n(\text{guest})$ (squares) and the free ligand *L* (circles). Reprinted with S.H. Cho, B.Q. Ma, S.T. Nguyen, J.T. Hupp and T.E. Albrecht-Schmitt, *Chem. Commun.*, 2563–2565. Copyright (2006) Royal Society of Chemistry

enantioselective performance of the free molecular analogue. Catalytic metal sites have also been incorporated as extra-framework species, an example being the encapsulation and stabilisation of free base metalloporphyrins into rho-ZMOF.^[165] Among these encapsulated phases, the Mn-metallated 5,10,15,20-tetrakis(1-methyl-4-pyridinio)porphyrin analogue shows catalytic activity toward the oxidation of cyclohexane with very high turnover numbers and cyclability.

Post-synthetic incorporation of metal sites into MOFs has proven to be a particularly powerful technique for generating reactive surfaces that would otherwise be inaccessible.^[35, 59, 71, 163] Of particular note here is the generation of a chiral framework that displays enantioselective catalytic activity,^[35] achieved in two synthetic steps: first, the synthesis of a chiral nanoporous phase $[\text{Cd}_3\text{Cl}_6\text{L}_3]\cdot n(\text{guest})$ ($L = (R)\text{-}6,6'\text{-dichloro-}2,2'\text{-dihydroxy-}1,1'\text{-binaphthyl-}4,4'\text{-bipyridine}$); and, second, the chemisorption of titanium(IV) isopropoxide sites onto the hydroxyl units of the chiral bridging ligands of the apohost. The resulting solid was found to catalyse ZnEt_2 additions to aromatic aldehydes with efficiencies and enantioselectivities comparable with those for the free $\text{Ti}(\text{O}^i\text{Pr})_2$ -functionalised BINOL-type ligand.

Finally, in an approach analogous to that used for porous carbons and zeolites, highly robust MOFs have been used as surface supports for metal atoms and clusters.^[158] An example here is the chemical vapour deposition of various metals into MOF-5, yielding materials classified as metal@MOF-5 for which the nature of metal inclusion and the extent of exogenous loading is currently unknown. Of these, Cu@MOF-5 is active in the synthesis of methanol from syngas and Pd@MOF-5 catalyses the reduction of cyclooctene by hydrogen.^[166]

1.2.4.2.2 Other Surface Sites

Whilst metal centres have provided the majority of known catalytic sites in MOFs, organic units have also provided a number of compelling examples. The size-selective catalytic activity of POST-1, described in Sections 1.2.1.1.2 and 1.2.3.2, in the transesterification of alcohols is attributed to the presence of unprotonated pyridyl groups that project into the channels and which likely assist in the deprotonation of the alcohol reactants. Catalytic yields in excess of 77 % were achieved with an $ee = \sim 8$ % using this homochiral system.^[29]

The post-synthetic generation of Brønsted acid surface sites – a structural feature that is largely in conflict with the coordination conditions for framework synthesis – has also led recently to catalytic activity in MOFs. Protonation of the bound carboxylato groups within the

framework [Cu(L-asp)(bpee)_{0.5}] (L-asp = L-aspartate; bpee = 1,2-bis(4-pyridyl)ethylene) leads to a material that catalyses epoxide methanolysis with up to a 65 % yield and *ee* = 17 %.^[39] The strongly acidic nature of this material arises from the binding of the protonated carboxylato unit to Cu^{II}, which increases the proton acid strength *via* the stabilisation of the conjugate base. Notably, such an arrangement is inaccessible in the homogeneous phase, where protonation of the amino acid at either the COO or NH₂ site leads to its dissociation from the metal centre. Brønsted acid sites have also been achieved through grafting of protonated ethylenediamine units onto the bare Cr^{III} sites of MIL-101, yielding a material that is active in the condensation of benzaldehyde and ethyl cyanoacetate. Notably, the inclusion and subsequent gentle reduction of charge-balancing anionic metal complexes leads to the inclusion of catalytically active Pd nanoparticles within this framework.^[72]

1.3 INCORPORATION OF OTHER PROPERTIES

Whereas conventional porous solids act largely as selective scaffolds within which reversible guest-exchange and catalysis can occur, the synthetic control over the structure and composition of MOFs, in addition to providing the impressive array of host-guest properties outlined above, has notably allowed the incorporation of many other interesting chemical and physical functions into these lattices. Many of these functions have been achieved for the first time in porous media, yielding host lattices that are able to respond and interact with guest molecules in entirely new and ‘intelligent’ ways. These notably include a range of magnetic, electronic, optical and mechanical phenomena, with the achievement of these commonly requiring the development of specific materials design principles relating both to the individual molecular building units and to their arrangement within the framework lattices. Whilst many such phenomena have been known and investigated for some time, it has only been recently that their design principles have been extended to the formation of open porous frameworks, allowing the combination of these properties with reversible host-guest chemistry for the first time. A strong motivation for these efforts has been the derivation of detailed structure-property relationships, with the exchange of guests providing both a powerful and very convenient means through which framework structure and, therefore, the property of interest can be perturbed systematically. For many of these properties the influence of exchangeable guest on host lattice function has

been found to be highly pronounced, offering potential scope in areas such as molecular sensing. Moreover, the recognition that unique synergies may exist between framework function and guest-exchange has led to the generation of materials with exotic new materials properties, including direct interplay between the various chemical and physical functions.

1.3.1 Magnetic Ordering

1.3.1.1 Overview

The accomplishment of magnetic exchange-coupling in coordinately linked frameworks has been investigated in detail since the early 1900s^[167–170] and, as such, has been both a pioneering and enduring motivation for the study of this class of materials. There are two principal approaches for the achievement of magnetic ordering in these systems: (1) the linkage of transition or lanthanoid metal ions through diamagnetic bridging ligands to achieve coupling between the metal spins; and (2) the linkage of these ions through radical ligands in which coupling between metal and ligand spins occurs. In each case the dimensionality of the framework lattice has important implications on the magnetic properties, as do issues such as the extent and nature of the coupling and the magneto-anisotropy of the metal ion. In each approach, the extent of exchange coupling and, therefore, magnetic ordering temperature commonly decreases rapidly as the number of bridging atoms between spin centres increases. Whereas many pure metals order magnetically at temperatures over 1000 K and metal oxide systems up to 900 K, those for two-atom bridged phases are below 350 K, whilst those for three-atom bridged frameworks^[171] do not exceed 50 K. At atomic separations beyond this the ordering temperatures typically drop to below 2 K.^[172] The investigation of coordinatively linked systems has therefore focused on a range of short bridges, which notably include hydroxo, cyanido, carboxylato, azido, dicyanamido, oxalato, and oxamato ligands. In contrast, the incorporation of radical ligands into framework lattices, which has received considerably less attention than the diamagnetic ligand approach due in part to their more difficult syntheses, allows the greater separation of metal ions to yield comparable magnetic ordering temperatures.

Given the very considerable literature on molecule based magnets (MBMs), which includes a number of detailed books and reviews,^[13, 167–169, 172] principal attention here is given to describing the recent emergence of porous magnets.

1.3.1.2 Porous Magnets

A considerable challenge in the formation of porous magnets lies in their dual requirement of magnetic exchange and interconnected pore volume. Whereas porosity in MOFs commonly requires the use of relatively long molecular connecting units, long-range magnetic ordering above millikelvin temperatures requires relatively short exchange pathways between nearest neighbour spin sites. Efforts to combine these seemingly inimical requirements within the one material have therefore focused on 2D and 3D framework compounds constructed through the bridging of certain transition metal ions with one- or two-atom bridges (*e.g.* hydroxo, carboxylato and cyanido, phosphonato, halido) or through the use of radical bridging ligands.^[13] An important requirement in such syntheses is the achievement of neutral framework lattices, with many early examples of open magnetic frameworks being nonporous on account of their pores being filled with counterions; examples here include systems with oxalato^[173–175] and formato,^[176, 177] bridges. Following early reports of ‘magnetic sponges’ that change their magnetic ordering properties upon irreversible guest desorption,^[178] these approaches have generated a number of novel porous magnetic phases. Whilst most of these have arisen through dedicated syntheses, some have notably derived from materials that have been known for many years, for which the guest-exchange capabilities were either unappreciated or regarded as an experimental inconvenience rather than a property worthy of exploitation.

In the absence of any success to date in the formation of metal oxides that are both magnetic and porous to molecular (as opposed to ion) inclusion, the main success in the use of one-atom bridges has been in the formation of hybrid materials containing the μ_3 -hydroxide and formate bridges. Principal among two-atom bridged materials are a range of metal cyanides, with Prussian Blue phases providing the majority of these. The emergence of these porous magnets^[13, 172, 179–188] has been important in allowing the investigation of both guest-induced perturbation of magnetic properties^[180–183, 185, 188] and magnetic-exchange interactions between host and guest.^[184] Further, the discovery of solvatomagnetic effects in such materials has been of particular interest, both for the systematic elucidation of magnetostructural relationships and for possible applications in areas such as molecular sensing.

1.3.1.2.1 Hybrid Metal Hydroxide Frameworks

In utilising hydroxo bridges between metal ions, approaches have focused principally on the use and modification of the brucite $M(\text{OH})_2$ structure,

which consists of edge-shared layers of octahedral transition metal ions (CdI₂-type), and the rutile-type structure, in which both edge- and vertex-sharing of metal octahedra occurs.^[172] Among a range of different modifications to the brucite parent structure are the formation of 1D edge-shared chains and the interruption of the layer through removal of some of the metal sites. Bridging or pillaring of these low dimensionality magnetic chains and layers with a range of multitopic organic ligands has then led in some cases to the formation of porous 3D framework lattices. Notable also has been the report of a 3D fully hydroxo-bridged lattice, [Co₅(OH)₂(OAc)₈].2H₂O, which displays canted antiferromagnetic behaviour below 30 K.^[189]

Among a large number of 1D hydroxo-bridged hybrid magnets^[172] is the squarate-bridged 3D framework [Co^{II}₃(OH)₂(C₄O₄)₂].3H₂O,^[190] which consists of 1D [Co^{II}₃(μ₃-OH)₂]⁴⁺ brucite-type ribbons linked by squarate anions to form a porous 3D network that houses 1D water-filled channels of dimensions 4.0 × 6.7 Å. Upon reversible dehydration/rehydration, single crystal diffraction measurements indicate that the framework experiences only minimal changes in its unit cell parameters and bond distances and angles, with a remarkable accompanying interconversion from antiferromagnetic to ferromagnetic ordering at 8 K (Figure 1.14).^[191] It is not currently known whether this pronounced change in magnetic properties results from the steric perturbation of the framework lattice, in which dehydration leads to a *ca* 2° change in some of the squarate binding angles, or whether magnetic-exchange coupling

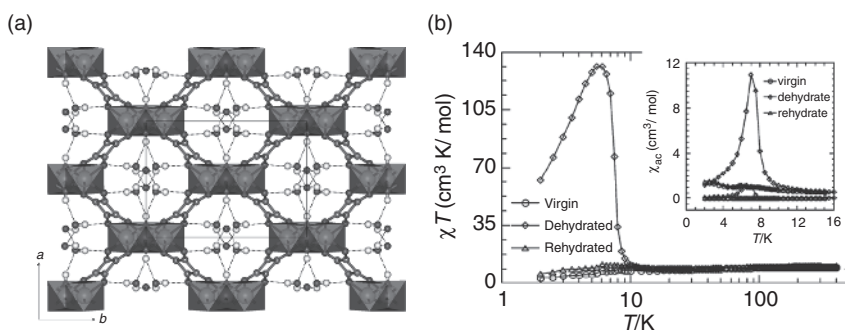


Figure 1.14 Structure of [Co^{II}₃(OH)₂(C₄O₄)₂].3H₂O (a) and guest-dependent magnetic behaviour (b), showing the DC susceptibility χT product and AC susceptibility (inset) for the virgin hydrated, dehydrated, and rehydrated frameworks. Reprinted with permission from S.O.H. Gutschke, D.J. Price, A.K. Powell and P.T. Wood, *Angew. Chem. Int. Ed.*, 38, 1088. Copyright (1999) Wiley-VCH Verlag GmbH & Co. KGaA.

through the hydrogen-bonding pore water molecules in the hydrated phase has some influence. Notable other 1D systems include a number of hybrid magnets based on the edge- and vertex-shared [110] ribbon within the rutile structure, having general formula $[M_3(\text{OH})_2(\text{dicarboxylate})_2(\text{H}_2\text{O})_4] \cdot n(\text{guest})$ ($M = \text{Co}, \text{Ni}, \text{Mn}$). These materials similarly order magnetically in the vicinity of 10 K, with the Co and Ni chains commonly forming ferrimagnets. A particularly notable example among these is the 3D framework $[\text{Ni}_3(\text{OH})_2(\text{cis-1,4-cyclohexanedicarboxylate})_2(\text{H}_2\text{O})_4] \cdot 2\text{H}_2\text{O}$, which contains 1D water-filled pores and converts from ferrimagnetic (2.1 K) to ferromagnetic ordering (<4.4 K) upon partial dehydration and rehydration.^[192]

More open porous frameworks containing 1D chains have been achieved through the bridging of metal centres by both oxide/hydroxide and carboxylate linkers. Two examples of such materials are the pseudo-isostructural $[\text{V}^{\text{IV}}\text{O}(\text{bdc})] \cdot n(\text{guest})$ (MIL-47)^[193] and $[\text{Cr}^{\text{III}}(\text{OH})(\text{bdc})] \cdot n(\text{guest})$ (MIL-53(Cr)),^[194] in which 1D channels of dimensions $7.9 \times 12 \text{ \AA}$ run parallel to the 1D metal chains. Whilst strong magnetic coupling is achieved in each material, the ordering is antiferromagnetic, with Néel temperatures (T_{NS}) for the as-synthesised phases of 95 K (MIL-47) and 65 K (MIL-53(Cr)). Guest desorption leads to pronounced flexibility, with the pores of V analogue opening to have dimensions $10.5 \times 11.0 \text{ \AA}$, and a shift in the T_{NS} to 75 K (MIL-47) and 55 K (MIL-53(Cr)·H₂O).

In the search for higher dimensionality magnetic pathways in the formation of porous phases some success has been achieved also in use of 2D hydroxo-bridged layers. Whereas the metal sites within the parent brucite-type $\text{Co}(\text{OH})_2$ structure (which is metamagnetic with $T_{\text{N}} = 10 \text{ K}$) are fully coordinated with an octahedral environment, variation in the synthesis conditions has allowed the replacement of some fraction of these sites with tetrahedral sites that lie out of the 2D layer and, in some cases, the replacement of hydroxo units with other μ_3 -bridging anions.^[172] The tetrahedral Co^{II} sites provide tethering points above and below the layer through which pillaring with bis-unidentate ligands has been achieved to produce materials with interlayer solvent-filled galleries. An example is the $[\text{Co}_8(\text{OH})_{12}(\text{SO}_4)_2(\text{diamine})] \cdot n\text{H}_2\text{O}$ family (diamine = 1,2-ethylenediamine (en), $n = 3$; diazabicyclooctane (dabco), $n = 1$), in which layer neutrality is achieved through replacement of 1 in 7 of the octahedral Co^{II} sites with two tetrahedral sites and 1 in 7 of the hydroxide sites with sulfate.^[179, 180] Diamine bridges then link the layers, with the ethylenediamine analogue displaying intercalative properties with interlayer collapse upon guest desorption, whereas the dabco analogue

displays robust porosity. Both display metamagnetic properties, with the higher ordering temperature of the dabco phase ($T_N = 21$ K, *cf.* 14 K for the en phase) attributed to the greater exchange coupling through the triple pathway of the dabco pillar. A distinct but related layer is seen in $[\text{Co}_5(\text{OH})_8(\text{chdc})] \cdot 4\text{H}_2\text{O}$ (chdc = *trans*-1,4-cyclohexanedicarboxylate), in which 1 in 5 of the octahedral Co^{II} sites are replaced with tetrahedral sites and charge neutrality of the framework is achieved through the use of a dicarboxylate pillar (see Figure 1.15).^[195] This material is ferrimagnetic with critical temperature, $T_c = 61$ K, implying ferromagnetic coupling between the layers, and has a very high coercive field of 22 kOe at 2 K.

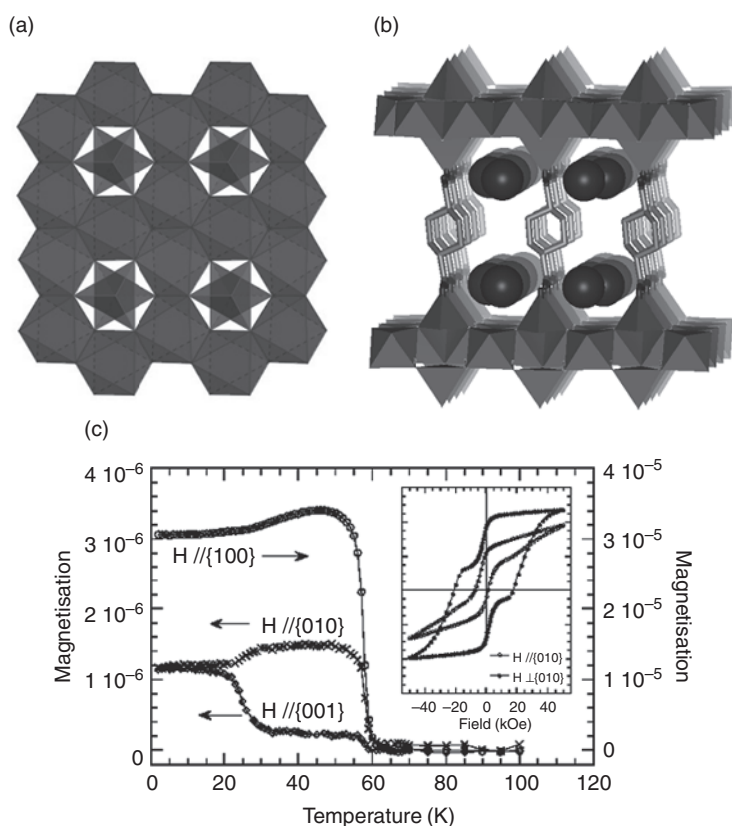


Figure 1.15 (a) Projection of the $\text{Co}_5(\text{OH})_8\text{L}_2$ layer, consisting of edge-shared octahedral Co^{II} and vertex-shared tetrahedral Co^{II} . (b) Pillared layer structure of $[\text{Co}_5(\text{OH})_8(\text{chdc})] \cdot 4\text{H}_2\text{O}$. (c) Temperature and field (inset; measured at 2 K) dependent magnetisation of $[\text{Co}_5(\text{OH})_8(\text{chdc})] \cdot 4\text{H}_2\text{O}$, measured with respect to the crystallographic axes. Reprinted with permission from M. Kurmoo, H. Kumagai, S.M. Hughes and C.J. Kepert, *Inorg. Chem.*, **42**, 6709. Copyright (2003) American Chemical Society

The higher magnetic ordering temperature of this phase over that of related systems is attributable to the higher proportion of tetrahedral Co^{II} sites.^[172] Upon dehydration the material undergoes a reversible single-crystal-to-single-crystal transformation in which the pillars rotate and the interlayer separation decreases slightly. This pronounced transformation has little observable influence on the magnetic properties.

1.3.1.2.2 *Metal Formates*

Whereas carboxylate units most commonly link metal ions through a three-atom bridge, it is not uncommon for these units to bridge two ions through a single oxygen atom. Whilst considerable magnetic exchange coupling may be achieved in the former case, particularly if multiple carboxylate bridges are present,^[196] the latter binding mode has been exploited to great effect in a family of formate-bridged frameworks of formula $[\text{M}_3(\text{HCOO})_6] \cdot n(\text{guest})$ (where $\text{M} = \text{Fe}, \text{Mn}, \text{Co}$ and Ni ; and $\text{guest} =$ a wide range of solvents) (see also Section 1.2.3.1.1 and Figure 1.11).^[140, 197–203] The framework topology of this family is that of a distorted diamond-type, in which each formate coordinates to three metal ions and each metal is linked to its nearest neighbours by one single oxygen atom of the formate and one three-atom carboxylate bridge. Guest desorption from this phase can be achieved with retention of the framework structure, with subsequent adsorption with other guests leading to pronounced breathing effects in which the lattice has been seen to expand in volume by up to 12 %. Despite the extended network of M-O-M linkages throughout the structures of these phases, the magnetic ordering temperatures are rather modest, with the maximum being 22 K for the ferromagnetic Fe analogue. As expected given the considerable structural perturbation seen with guest exchange, the magnetic properties of these systems are highly variable, with the ordering temperature of the Fe analogue lying in the range 15–22 K depending on the identity of the adsorbed guest.

1.3.1.2.3 *Metal Cyanides*

The Prussian Blue family of materials, in addition to providing the first coordination compound back in 1704, has provided and continues to provide a wide range of interesting magnetic behaviours.^[204–206] The family consists of a diverse array of frequently misassigned structures of general formula $\text{C}_m\text{A}_x[\text{B}(\text{CN})_6]_y \cdot n\text{H}_2\text{O}$ (where $\text{C} =$ cation, *e.g.* K^+, Cs^+ ; A and $\text{B} =$ octahedral transition metal ions). Examples include Prussian Blue itself, $\text{Fe}^{\text{III}}_4[\text{Fe}^{\text{II}}(\text{CN})_6]_3 \cdot 14\text{H}_2\text{O}$, in which vacancies at the ferrocyanide sites within the cubic network rather than cation inclusion lead to charge balance, and a range of other vacancy ($\text{A}_x[\text{B}(\text{CN})_6]_y \cdot n\text{H}_2\text{O}$; $x \neq y$)

and nonvacancy ($C_m A[B(CN)_6] \cdot nH_2O$; $0 \leq m \leq 2$) phases. Following the report of ferromagnetic ordering at 5.6 K in Prussian Blue in 1928,^[207] the magnetic ordering temperatures of these frameworks have been increased through the variation of metal ions and framework composition. Following early work in which the diamagnetic low spin Fe^{II} sites within Prussian Blue were replaced with paramagnetic metal ions, more strategic efforts have been directed towards optimising the sign and magnitude of the magnetic exchange coupling through variation of the orbital occupancies (*e.g.* making use of the ferromagnetic $t_{2g}(B)-e_g(A)$ pathway) and relative energies. Notable successes from this strategy include $CsNi^{II}[Cr^{III}(CN)_6] \cdot 2H_2O$ (90 K ferromagnet),^[208] $Cs_{0.75}Cr^{II}_{1.125}[Cr^{III}(CN)_6] \cdot 5H_2O$ and $Cr^{II}_3[Cr^{III}(CN)_6]_2 \cdot 10H_2O$ (190 K and 240 K ferrimagnets, respectively),^[209] $V^{II}_{0.42}V^{III}_{0.58}[Cr^{III}(CN)_6]_{0.86} \cdot 2.8H_2O$ (315 K ferrimagnet),^[210] $K_{0.058}V^{II/III}[Cr(CN)_6]_{0.79} \cdot (SO_4)_{0.058} \cdot 0.93H_2O$ (372 K ferrimagnet),^[211] and $KV^{II}[Cr^{III}(CN)_6] \cdot 2H_2O$ (376 K ferrimagnet).^[212] The achievement of room temperature ordering in the latter V/Cr systems, albeit with very small coercive fields (*e.g.* 25 Oe at 10 K for $V^{II}_{0.42}V^{III}_{0.58}[Cr^{III}(CN)_6]_{0.86} \cdot 2.8H_2O$ ^[210]), represents a major advance. A second broad family of cyanide-bridged magnets are bimetallic systems in which the hexacyanidometallate $[B(CN)_6]^{m-}$ metalloligands are linked through coordinatively unsaturated $[A(L)_x]^{m-}$ units (where L = polyamine ligands for example).^[213] Early examples from this family include $[Ni(en)_2]_3[Fe(CN)_6]_2 \cdot 2H_2O$ ($en = 1,2$ -ethylenediamine), which contains a ladder-type $Ni^{II}-Fe^{III}$ network that orders ferromagnetically at 18.6 K,^[214] and $[Mn(en)]_3[Cr(CN)_6]_2 \cdot 4H_2O$, which consists of a 3D $Mn^{II}-Cr^{III}$ network that orders ferrimagnetically at 69 K.^[215]

Of the relatively small number of reports of reversible guest-exchange in cyanide-based magnets, the Prussian Blue family provides many interesting examples. Following the demonstration of robust porosity in this family of materials,^[216-219] it has been found that reversible water desorption from $CsNi^{II}[Cr^{III}(CN)_6] \cdot 2H_2O$ and $Cr^{II}_3[Cr^{III}(CN)_6]_2 \cdot 10H_2O$ leads to apohost phases with BET surface areas of 360 and 400 $m^2 g^{-1}$ and magnetic ordering temperatures of $T_c = 75$ K and $T_N = 219$ K, respectively;^[184] these are only slightly decreased from those of the hydrated phases (see above), with the latter being the highest ordering temperature yet observed for a porous magnet. Upon adsorption of the paramagnetic O_2 guest molecule, opposite magnetic couplings between host and guest are seen for each material; for $CsNi^{II}[Cr^{III}(CN)_6]$, there is an increase in the magnetic moment, indicating ferromagnetic exchange, whereas for $Cr^{II}_3[Cr^{III}(CN)_6]_2$ there is a reduction of the coercivity from 110 to 10 G and of the remnant magnetisation from 1200 to 400 emu

G mol^{-1} , indicating antiferromagnetic exchange. Notably, through examination of the O_2 adsorption energetics it was concluded that the magnetic interaction has at most a negligible influence on the adsorption energetics, suggesting that the proposed exploitation of internal magnetic field for the separation of O_2 from air is unrealisable.

In related systems, solvatomagnetic effects have been reported in the vacancy phase $\text{Co}^{\text{II}}_{1.5}[\text{Cr}^{\text{III}}(\text{CN})_6] \cdot 7.5\text{H}_2\text{O}$, which converts from a peach-coloured and ferromagnetically coupled ($T_c = 25 \text{ K}$) solid to a blue and antiferromagnetically coupled phase ($T_N = 18 \text{ K}$) of formula $\text{Co}^{\text{II}}_{1.5}[\text{Cr}^{\text{III}}(\text{CN})_6] \cdot 2.5\text{H}_2\text{O} \cdot 2\text{EtOH}$ on exposure to ethanol, an effect attributed to a change from six- to (average) four-coordination at the Co^{II} centre.^[220] A similar effect is seen with the systematic variation of water occupancy in $\text{Co}[\text{Cr}(\text{CN})_6]_{2/3} \cdot n\text{H}_2\text{O}$, which upon reversible desorption of bound and unbound water guests converts from pink with octahedral Co^{II} to blue with tetrahedral Co^{II} ; accompanying this humidity-dependent transformation is a change from ferromagnetic to antiferromagnetic coupling and a decrease in the magnetic ordering temperature from 28 to 22 K (see Figure 1.16).^[221] A more pronounced change in ordering temperature is seen in $\text{K}_{0.2}\text{Mn}_{1.4}\text{Cr}(\text{CN})_6 \cdot 6\text{H}_2\text{O}$, where T_N increases from 66 to 99 K upon water desorption.^[222]

A number of more structurally diverse cyanide-bridged materials have also been shown to display reversible solvatomagnetic effects. These include the flexible host lattice $[\text{Mn}(\text{NNdmenH})(\text{H}_2\text{O})][\text{Cr}(\text{CN})_6] \cdot \text{H}_2\text{O}$ ($\text{NNdmen} = N,N$ -dimethylethylenediamine), which undergoes a reversible single-crystal-to-single-crystal transformation from the 2D layer structure of the parent phase to a 3D pillared-layer framework, $[\text{Mn}(\text{NNdmenH})][\text{Cr}(\text{CN})_6]$, a transformation that involves the generation and cleavage of Mn-N bonds. This structural change leads to an increase in the ferrimagnetic ordering temperature from 35.2 to 60.4 K.^[223] Among a range of interesting porous phases based on the $S=1/2$ octacyanidotungstate(V) unit, pronounced solvatomagnetism is seen in the 2D framework $[\text{Ni}(\text{cyclam})]_3[\text{W}(\text{CN})_8]_2 \cdot 16\text{H}_2\text{O}$ ($\text{cyclam} = 1,4,8,11$ -tetraazacyclotetradecane), which converts from ferromagnetic behaviour to canted ferromagnetic upon reversible dehydration; this effect is attributed to a large change in the Ni-NC-W angles.^[224] Similarly, exchange of water for *n*-propanol in the 3D framework $\text{Cu}_3[\text{W}(\text{CN})_8]_2(\text{pmd})_2 \cdot 8\text{H}_2\text{O}$ ($\text{pmd} = \text{pyrimidine}$) to form $\text{Cu}_3[\text{W}(\text{CN})_8]_2(\text{pmd})_2 \cdot 1.5\text{PrOH} \cdot 2.25\text{H}_2\text{O}$ results in an increase in magnetic ordering temperature from 9.5 to 12.0 K and a dramatic increase in coercive field; these changes are attributed to a decrease in antiferromagnetic coupling to a Cu site that converts from 6- to 5-coordinate.^[225]

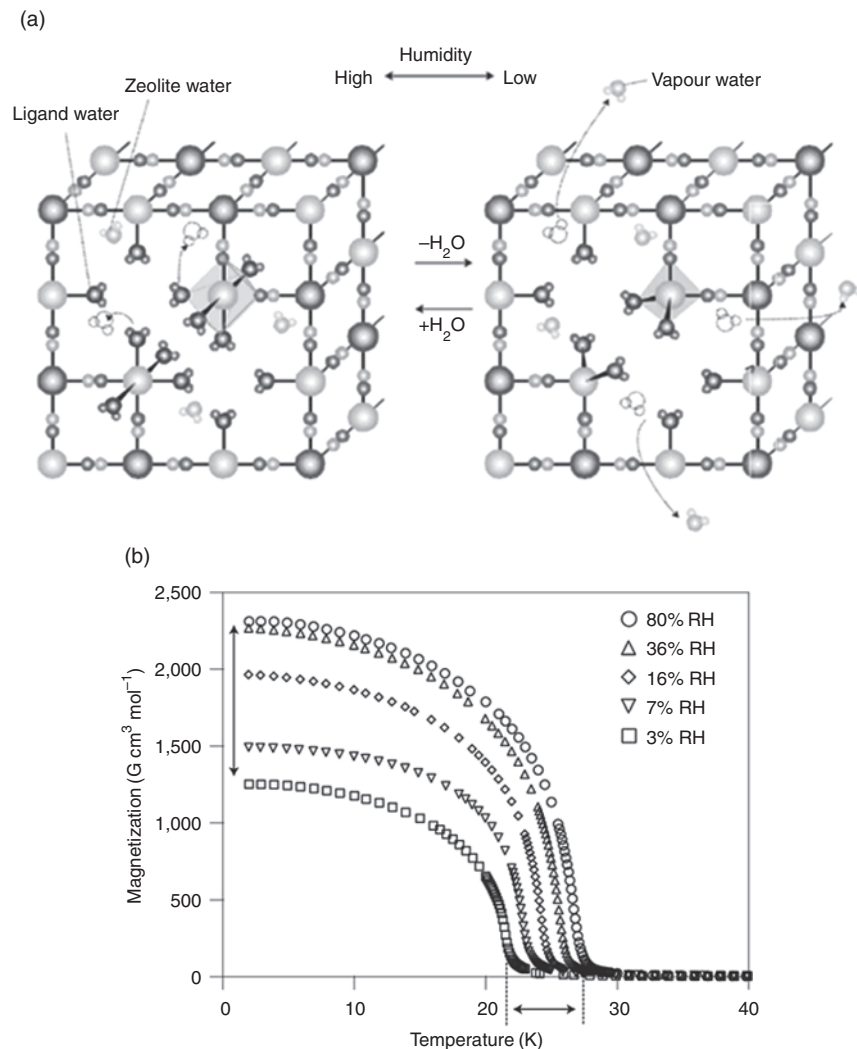


Figure 1.16 Adsorption and desorption of bound and unbound water from the vacancy Prussian Blue $\text{Co}[\text{Cr}(\text{CN})_6]_{2/3} \cdot n\text{H}_2\text{O}$ (a) and the influence of relative humidity (RH) on magnetic ordering temperature, as seen in the low temperature magnetisation (b). Reprinted with permission from S.I. Ohkoshi, K.I. Arai, Y. Sato and K. Hashimoto, *Nat. Mat.*, 3, 857. Copyright (2004) Nature Publishing Group

1.3.1.2.4 Radical ligands

Principal attention in the incorporation of radical multitopic ligands into MOF phases has focused on the well known π -acceptors TCNE (tetracyanoethylene) and TCNQ (7,7,8,8-tetracyanoquinodimethane), which in their mononegative forms have an unpaired spin that can couple with

spins on metal ions to which they are coordinated.^[226] Among a range of framework materials constructed with these ligands is the amorphous room temperature magnet $V[TCNE]_x \cdot nCH_2Cl_2$ ($x \sim 2$; $n \sim 0.5$), which is proposed to have a glass-like 3D framework structure of the form $V^{II}[TCNE]_z [TCNE]^{2-}_{1-z/2}$ ($1 < z < 2$). This material orders magnetically at 125 °C, which is marginally higher than the Prussian Blue phases. The same radical 4-connecting linker is seen in the phases $[Fe(TCNE^-)(C_4(CN)_8)_{1/2}] \cdot nCH_2Cl_2$ ^[227] and $[Fe^{II}(TCNE^-)(NCMe)_2]^+[Fe^{III}Cl_4]^-$,^[228] the structures of which were determined by synchrotron powder diffraction measurement. These materials order magnetically in the vicinity of 100 K. Among a number of chemically functionalised TCNQ-based framework magnets are the 2D layered framework $[(Ru_2(O_2CCF_3)_4)_2(TCNQF_4)] \cdot 3$ (*p*-xylene), which orders magnetically at 95 K,^[229] and the 3D Ru framework $[(Ru_2(O_2CPh-*m*-F)_4)_2(BTDA-TCNQ)]$ (where BTDA-TCNQ = bis(1,2,5-thiadiazolo)tetracyanoquinodimethane), which is a ferromagnet with $T_c = 107$ K.^[230] Host-guest properties have yet to be reported for a porous TCNE or TCNQ based magnet, with the closest example being the demonstration of reversible guest-exchange in a diamagnetic pillared layer phase $[Zn^{II}(TCNQ^{2-})(4,4'-bpy)] \cdot 6MeOH$.^[231] The radical ligand approach has, however, led to the successful generation of porous 2D frameworks constructed using the highly stable polychlorinated tris(4-carboxyphenyl)methyl (PTMTC) radical.^[182, 232, 233] Most notable among these is the highly flexible porous phase $[Cu^{II}_3(PTMTC)_2(py)_6(EtOH)_2(H_2O)]$ (MOROF-1; see Figure 1.17), which shrinks and expands by up to 30 vol% with ethanol desorption/adsorption and displays subtle solvatomagnetic effects associated with framework collapse and the removal of coordinated guests.^[182]

1.3.2 Electronic and Optical Properties

Among a wide range of electronic and optical phenomena known in molecular systems, many have been achieved and investigated in MOFs. As with the magnetic systems described above, recent efforts to incorporate such properties into porous systems have led to the first investigations of guest-induced perturbations of these phenomena, leading to a sensing function. Unlike porous magnets, for which magnetostriction effects are generally negligible, a further particular interest here lies in the often highly pronounced coupling of electronic excitation with lattice energetics, leading to direct interplay between electronic/optical and host-guest function.

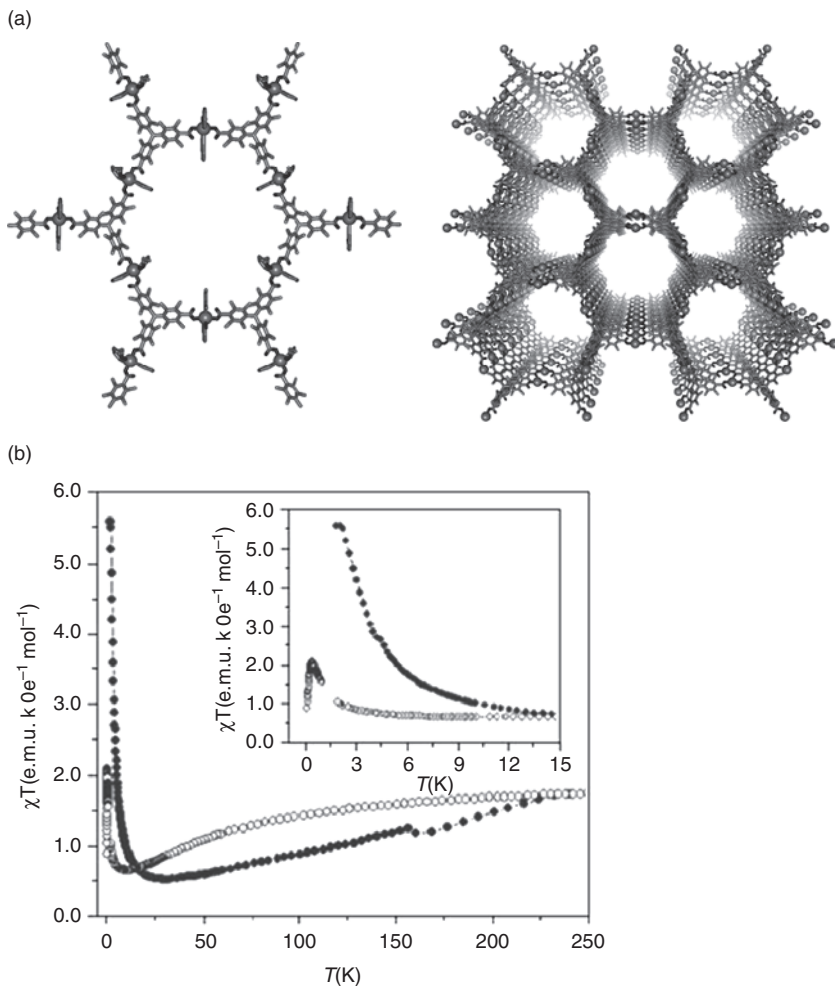


Figure 1.17 (a) Structure of MOROF-1, which consists of 2D hexagonal layers in which Cu^{II} ions are bridged by the radical $S = 1/2$ ligand PTMTC. (b) χT product for the solvated (filled circles) and desorbed (open circles) framework. Reprinted with permission from D. Maspoch, D. Ruiz-Molina, K. Wurst, N. Domingo, M. Cavallini, F. Biscarini, J. Tejada, C. Rovira and J. Veciana, *Nat. Mater.*, 2, 190. Copyright (2003) Nature Publishing Group

1.3.2.1 Spin crossover

Spin crossover (SCO) in transition metal compounds is a well known form of molecular bistability in which the transition between a low-spin (LS) and a high-spin (HS) state can be induced by a variation of temperature, pressure, magnetic field or light irradiation. Physical consequences

of this transition include pronounced changes in colour, magnetic moment, and coordination bond distances and strengths. The observation of abrupt transitions and memory effects in SCO materials, which arise due to electron–phonon coupling between the SCO sites and long-range elastic interactions within the lattice,^[234] has led to suggestions that these materials may be candidates for application in information storage and retrieval, temperature sensing and visual displays.^[235]

Early efforts to incorporate this electronic molecular switch into framework materials were driven primarily by an interest in elucidating the nature of cooperativity in SCO lattices, with the ultimate goal of controlling the switching properties to deliver bistable systems at ambient temperature.^[236–248] Classical examples of such systems are members of a family of 1,2,4-triazole bridged 1D chain compounds of type $[\text{Fe}^{\text{II}}(\text{R-trz})_3](\text{anion})_2$, which undergo abrupt SCO transitions and wide thermal hysteresis loops ($\Delta T = 35 \text{ K}$) spanning room temperature.^[235–237] Elaboration of the ligand design to include alkane-linked bis-triazoles (btr) and bis-tetrazoles (btzb) subsequently yielded compounds of types $[\text{Fe}(\text{btr})_2(\text{NCS})_2] \cdot \text{H}_2\text{O}$ ^[243] and $[\text{Fe}(\text{btzb})_3](\text{ClO}_4)_2$,^[248] which have 2D and 3D framework structures, respectively, and quite diverse SCO behaviour with hysteresis present in some cases. Cyanidometallate bridges between SCO centres have also led to pronounced hysteresis near ambient temperature, most notably in the 2D layered Hofmann type materials $[\text{Fe}(\text{py})_2\text{M}(\text{CN})_4]$ ($M = \text{Ni}, \text{Pd}, \text{Pt}; \text{py} = \text{pyridine}$)^[249] and the 3D pillared Hofmann frameworks $[\text{Fe}(\text{pz})\text{M}(\text{CN})_4] \cdot 2(\text{H}_2\text{O})$ ($\text{pz} = \text{pyrazine}$), which have ΔT up to 33 K.^[240] Among other rare examples of 3D SCO framework phases is the Prussian Blue analogue, $\text{CsFe}^{\text{II}}[\text{Cr}^{\text{III}}(\text{CN})_6]$, which undergoes SCO both thermally^[250] and upon irradiation with X-rays.^[251]

The recent achievement of porosity in SCO frameworks provides a new approach for investigating features such as the ligand field, electronic and steric communication between SCO centres, and lattice dynamics, as well as providing materials with completely new host-guest properties.^[252] Among a range of porous spin crossover frameworks (SCOFs) are an extensive isotopological family of the form $[\text{Fe}(\text{L})_2(\text{NCX})_2] \cdot n(\text{guest})$ ($\text{L} = \textit{trans}$ -1,2-bis(4-pyridyl)ethene (tvp, also bpee),^[239] 4,4'-azopyridine (azpy),^[197] 1,2-bis(4-pyridyl)ethane (bpe),^[253] 1,2-bis(4'-pyridyl)-1,2-ethanediol (bped),^[254] and 2,3-bis(4'-pyridyl)-2,3-butanediol (bpbd),^[255, 256] and $\text{X} = \text{S}, \text{Se}$), which consist of interpenetrated rhombic grids between which 1D channels lie.^[254] Investigation of the guest-exchange chemistry of the azpy, bpe, bpbd and bped analogues has uncovered a range of subtle guest-dependent structural and

electronic behaviours. The azpy analogue, $[\text{Fe}^{\text{II}}_2(\text{azpy})_4(\text{NCS})_4] \cdot n(\text{guest})$, displays a broad half SCO transition that depends on the nature of guest inclusion. Desorption of the unbound ethanol guests of the parent phase leads to a transformation in which the 1D pore channels collapse partially, with the open framework geometry being returned with the adsorption of a range of different alcohol guests. The guest-loaded phases display subtly different SCO properties, whereas the apohost is HS to low temperature; removal of the SCO function is attributed to the weakening of the Fe^{II} ligand field caused by nonideal coordination geometries following guest removal.^[97] The bped analogue was the first porous material in which pore environment can be varied by excitation by light. The SCO in this material, which may also be induced thermally and/or influenced by the desorption/sorption of guest ethanol molecules, leads to a subtle breathing of the framework structure and modification of the pore chemistry.^[253] The bpe analogue, $[\text{Fe}(\text{bpe})_2(\text{NCS})_2] \cdot n(\text{guest})$, displays a guest- and spin-state dependence of considerable complexity. Through variable temperature synchrotron powder and single crystal X-ray diffraction measurement, coupled with characterisations of the host-guest, magnetic and photomagnetic properties, it was shown that this material can exist in at least nine subtly distinct structural forms as a function of guest loading, temperature and light irradiation. These uniquely include a half-spin state in which there is a checkerboard arrangement of HS and LS Fe^{II} sites at the two-step plateau (see Figure 1.18).^[253] The most structurally robust of these phases incorporates the bpbld linker, with almost perfect framework rigidity resulting from a network of hydrogen-bonding interactions between the interpenetrated $[\text{Fe}(\text{bpbld})_2(\text{NCS})_2]$ grids. The switching temperature of this phase can be controlled in a predictable fashion by the incorporation of guests with differing polarities, an effect that emerges because the influence of steric interactions between host and guest are minimised. This material is unique among the SCOF family in displaying bistability, with thermal hysteresis in the SCO transition being attributed to the high degree of lattice cooperativity. Intriguingly, this can be turned on and off by the inclusion of different guests, indicating that host-guest rather than solely intraframework effects can influence the extend of lattice cooperativity and resulting memory effects in SCO systems.^[255]

The use of cyanidometallate linkers between SCO metal centres has also generated a range of interesting porous phases. One 3D example, $[\text{Fe}^{\text{II}}(\text{pmd})(\text{H}_2\text{O})(\text{M}^{\text{I}}(\text{CN})_2)_2] \cdot \text{H}_2\text{O}$ (pmd = pyrimidine; $\text{M}^{\text{I}} = \text{Ag}, \text{Au}$) displays the multifunctional properties of SCO, hysteresis ($\Delta T = 8 \text{ K}$) and a reversible dehydration/rehydration structural interconversion in

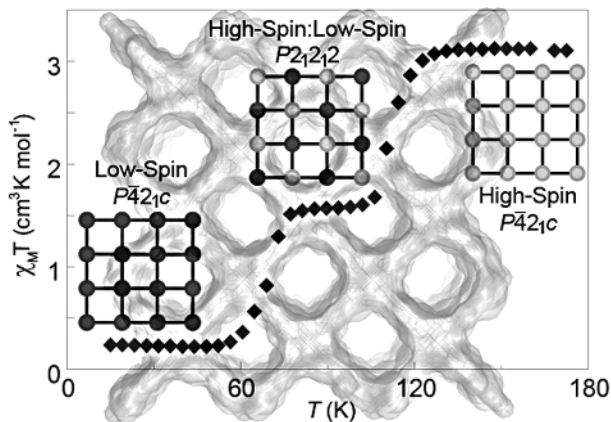


Figure 1.18 Two-step spin crossover in the interpenetrated square grid framework $[\text{Fe}^{\text{II}}(\text{bpe})_2(\text{NCS})_2] \cdot n(\text{guest})$ (SCOF-4; shown in the background viewed down the 1D pores). The switching in this porous system proceeds from fully high-spin (right) to fully low-spin (left) *via* a checkerboard-type arrangement of high-spin and low-spin Fe^{II} nodes (centre). Reprinted with permission from G.J. Halder, K.W. Chapman, S.M. Neville, B. Moubaraki, K.S. Murray, J.F. Létard and C.J. Kepert, *J. Am. Chem. Soc.*, **130**, 17552. Copyright (2008) American Chemical Society

the crystal phase, the latter yielding the substitution of H_2O for pmd at the Fe^{II} centres.^[106] This conversion results in large changes to the switching properties: for the Ag phase the SCO transition moves to lower temperature and has a larger hysteresis, whereas for the Au phase the transition is eliminated completely. In contrast, a very high degree of structural robustness has been found in the SCO Hofmann phases $[\text{Fe}^{\text{II}}(\text{pz})\text{M}^{\text{II}}(\text{CN})_4] \cdot 2(\text{H}_2\text{O})$ ($\text{M}^{\text{II}} = \text{Ni}, \text{Pd}, \text{Pt}$; $\text{pz} = \text{pyrazine}$), which consist of square grid $[\text{FeM}(\text{CN})_4]$ layers pillared by pyrazine (see Figure 1.19).^[240] Dehydration of the Pt analogue leads to an increase in both the temperature and width of the SCO hysteresis loop.^[257] Subsequent guest-dependent measurements on this family have uncovered a range of unprecedented materials properties, which include both guest-induced switching (providing a selective molecular sensing mechanism) and switch-induced changes to host–guest function (enabling manipulation of pore chemistry and therefore guest uptake/release through external stimuli).^[258, 259] Further, exploitation of the electronic bistability of this system allows these processes to occur with a degree of molecular memory; for example, the framework can be switched to its alternate state by adsorption then desorption of one guest, then switched back by use of a different guest. Adsorption measurements in the bistable

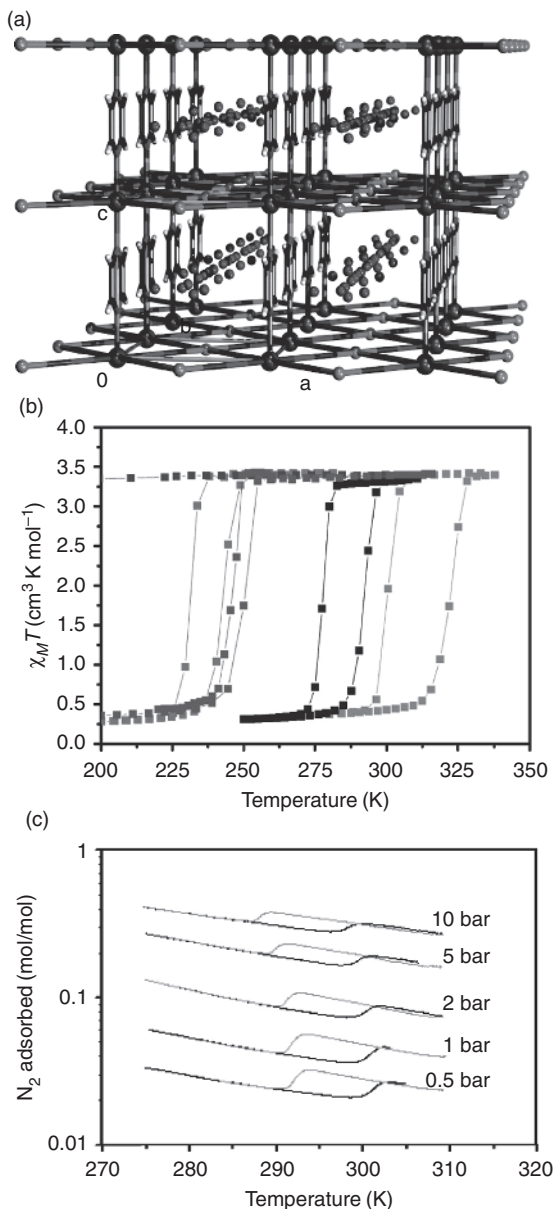


Figure 1.19 (a) Structure of $[\text{Fe}^{\text{II}}(\text{pz})\text{Ni}^{\text{II}}(\text{CN})_4] \cdot 2(\text{H}_2\text{O})$. (b) Influence of the adsorption of (from left to right) toluene, acetone, ethanol, methanol, and acetonitrile on the thermal SCO behaviour. (c) Dinitrogen isotherms collected on cooling (grey) and warming (black), showing the influence of the hysteretic spin transition on the gas adsorption properties. Reprinted with permission from P.D. Southon, L. Liu, E.A. Fellows, D.J. Price, G.J. Halder, K.W. Chapman, B. Moubaraki, K.S. Murray, J.F. Léard and C.J. Kepert, *J. Am. Chem. Soc.*, **131**, 10998. Copyright (2009) American Chemical Society

temperature region yield a range of unique behaviours. The HS and LS framework states display different guest affinities due to a *ca* 0.25 Å difference in pore dimension associated with the *ca* 0.2 Å difference in Fe-N bond lengths. Direct interplay between the host-guest and switching properties is also seen in adsorption isobar measurements, in which the hysteretic nature of the SCO is mirrored in the guest adsorption and desorption (see Figure 1.19).

1.3.2.2 Electron Transfer

The observation and investigation of electron transfer processes in MOFs pre-dates the exploration of porosity in these systems by some decades and, in the case of Prussian Blue, by more than two centuries. Among various types of electron transfer are a range of inner sphere processes, many corresponding to class II mixed valency^[260] in which thermal energies or photoexcitation are sufficient to excite electrons between the different centres within the framework. In principle, the combination of porosity and electron transfer represents one of the great current challenges in the field, with strong coupling between these effects expected to lead to interesting synergies. The achievement of electrically conducting porous phases, in particular, is of interest for possible applications in molecular sensing and selective electrode materials as well as a number of more advanced functions. With electron transfer being largely unexplored in porous framework phases, only brief attention to this property is given here.

Prussian Blue phases provide a range of examples where electron transfer occurs from metal to metal (intervalence charge-transfer, IVCT). Of particular interest is the influence of photo-induced transfer on magnetic properties. In $\text{K}_{0.2}\text{Co}_{1.4}[\text{Fe}(\text{CN})_6]\cdot 6.9\text{H}_2\text{O}$,^[261] IVCT can be tuned by irradiation with photons of different frequencies, with red light enhancing the magnetisation and increasing the ferrimagnetic ordering temperature from 16 to 19 K through electron transfer from Fe to Co. Blue light, or heating to 150 K, reverses this effect. Similarly, photo-excitation of paramagnetic $\text{Rb}_{0.66}\text{Co}_{1.25}[\text{Fe}(\text{CN})_6]\cdot 4.3\text{H}_2\text{O}$ ^[262] (with charge distribution $\text{Rb}_{0.66}\text{Co}^{\text{III}}_{0.84}\text{Co}^{\text{II}}_{0.41}[\text{Fe}^{\text{II}}(\text{CN})_6]$) yields a defect pair of Fe^{III} (LS) and Co^{II} (HS) that cause ferrimagnetic ordering at 15 K. Reversible photomagnetism has also been observed in rubidium manganese hexacyanidoferrates,^[263] with photo-demagnetisation in $\text{Rb}_{0.91}\text{Mn}_{1.05}[\text{Fe}(\text{CN})_6]\cdot 0.6\text{H}_2\text{O}$ occurring due to conversion from $\text{Fe}^{\text{II}}\text{-CN-Mn}^{\text{III}}$ to $\text{Fe}^{\text{III}}\text{-CN-Mn}^{\text{II}}$.^[264] A novel further property is that of photo-induced magnetic pole inversion,

seen in $(\text{Fe}_{0.40}\text{Mn}_{0.60})_{1.5}[\text{Cr}(\text{CN})_6] \cdot 7.5\text{H}_2\text{O}$.^[265] Octacyanidometallates ($M = \text{Mo}, \text{W}$) have also produced a number of interesting photo-active phases. Photo-excitation of $\text{Cu}_2[\text{Mo}(\text{CN})_8] \cdot 8\text{H}_2\text{O}$,^[266] leads to conversion from a paramagnet to a ferromagnet with $T_c = 25 \text{ K}$. Both temperature- and irradiation-induced IVCT are seen in $\text{Cs}[\text{Co}^{\text{II}}(3\text{-cyanopyridine})_2][\text{W}^{\text{V}}(\text{CN})_8] \cdot \text{H}_2\text{O}$ ^[267] and $\text{Co}^{\text{II}}_3[\text{W}^{\text{V}}(\text{CN})_8]_2(\text{pmd})_4 \cdot 6\text{H}_2\text{O}$ ($\text{pmd} = \text{pyrimidine}$) (see Figure 1.20),^[268] for which conversion from $\text{Co}^{\text{II}}(\text{HS}, S = 3/2) - \text{W}^{\text{V}}(S = 1/2)$ to $\text{Co}^{\text{III}}(\text{LS}, S = 0) - \text{W}^{\text{IV}}(S = 0)$ occurs with broad thermal hysteresis (167–216 K and 208–298 K, respectively). Reversal of this charge transfer with irradiation at low temperature yields metastable ferromagnets with ordering temperatures of 30 and 40 K, respectively.

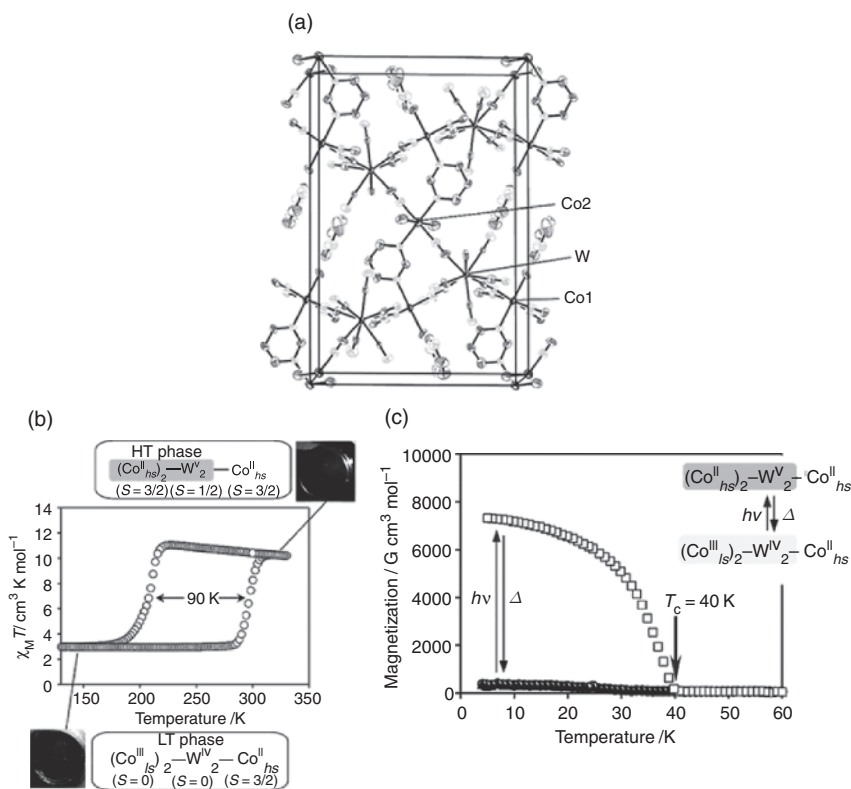


Figure 1.20 (a) Structure of $\text{Co}^{\text{III}}_3[\text{W}^{\text{V}}(\text{CN})_8]_2(\text{pmd})_4 \cdot 6\text{H}_2\text{O}$. (b) Thermal hysteresis in the thermal interconversion between $\text{Co}^{\text{II}} - \text{W}^{\text{V}}$ (high temperature) and $\text{Co}^{\text{III}} - \text{W}^{\text{IV}}$ (low temperature) forms. (c) Influence of photo-excitation at low temperatures on the magnetisation. Reprinted with permission from S. Ohkoshi, S. Ikeda, T. Hozumi, T. Kashiwagi and K. Hashimoto, *J. Am. Chem. Soc.*, **128**, 5320. Copyright (2006) American Chemical Society

In the parallel investigation of systems where metal-ligand charge-transfer (MLCT) occurs, studies into transition metal complexes of the redox-active quinone ligand have unravelled crossover behaviour that accompanies electron transfer.^[269] This reversible process, known as valence tautomerism, has been observed with bistability in the solid state.^[270] Exotic photomechanical behaviours, such as the bending of crystals of 1D chain materials with IR irradiation,^[271, 272] have been attributed to the unique structural consequences of electron transfer within the solid.

Whereas metal chalcogenides have made some important inroads into the challenge of generating electrically conducting porous phases,^[273] little to no progress has been made to date on the merging of these two properties in MOF systems, with only weakly conducting materials achieved. For example, measurements on the fully dehydrated Prussian Blue, $\text{Fe}_4[\text{Fe}(\text{CN})_6]_3$, indicate that the very modest semiconducting nature of this phase arises due to electron hopping between the Fe^{II} and Fe^{III} sites, a process that is also responsible for its intense blue colour. Electron delocalisation to give metallic conductivity is, however, well known in a number of nonporous phases. These include the Cu-DCNQI system (DCNQI = a range of *N,N*-dicyanoquinonediimines),^[274] in which electron delocalisation and metallic conductivity occur due to a close matching of donor-acceptor electronic energy levels and strong orbital overlap. Also of note are a range of layered organic/inorganic materials in which electrical conduction occurs within electron-delocalised organic layers, such as those containing the bis(ethylenedithio)tetrathiafulvalene (BEDT-TTF) donor molecule;^[275] examples here are the paramagnetic superconductor $(\text{BEDT-TF})_4\text{A}[\text{Fe}(\text{C}_2\text{O}_4)_3]\cdot\text{C}_6\text{H}_5\text{CN}$ ($\text{A} = [\text{H}_3\text{O}]^+, \text{K}^+, [\text{NH}_4]^+$)^[276] and the ferromagnetic metal $(\text{BEDT-TTF})_3[\text{MnCr}(\text{C}_2\text{O}_4)_3]$,^[277] each of which contain magnetic oxalate based layers between the conducting organic layers.

1.3.2.3 Photoluminescence

The high level of control over chemical structure conferred by metal-organic synthesis makes MOF materials a fertile area for the achievement of novel optical properties. Such properties include nonlinear optics (NLO), achieved through the generation of noncentrosymmetric frameworks, and luminescence, achieved through the strategic arrangement of photo-active metal ions and organic ligands. A motivation for the latter is that MOF formation commonly leads to local geometric constraints that can lead to increased quantum efficiencies and fluorescence lifetimes.

Most notably, particular recent attention has been given to the synthesis of materials that are both porous and luminescent due to an interest in solvato-optical properties.^[10, 13, 278, 279]

In addition to the processes described in Section 1.3.2.2 involving electron transfer between neighbouring metals (IVCT) and metal/ligand (MLCT and LMCT), luminescence can arise due to metal-based emission (*e.g.* for lanthanoid and d^{10} transition metal ions), ligand based emission (*e.g.* for conjugated organic linkers), guest molecule emission, and exciplex formation between host and guest.^[278] Each of these processes can be influenced strongly by the presence of adsorbed guest molecules, providing a sensitive mechanism for molecular sensing that in principle promises detection levels approaching the single-molecule limit.^[278]

The incorporation of luminescent lanthanoid nodes into framework lattices has led to a number of materials in which guest-dependent luminescence is seen. In the highly porous $[\text{Tb}_2(\text{tatb})_2(\text{dma})_3]$ (tatb = triazine-1,3,5-(4,4',4''-trisbenzoate); dma = *N,N*-dimethylacetamide), which is remarkable in containing 47 and 39 Å pores within a cubic lattice with cell parameter $a = 123.901(1)$ Å, adsorption of ferrocene molecules leads to a quenching of the Tb^{III} emission that is attributable to a nonradiative energy-transfer pathway between host and guest.^[47] Further, it was found in this system that emission from the included ferrocene guests was higher than that expected, suggesting that the framework acts as an antenna in harvesting photons for the guests. Similar reversible guest-induced quenching is seen with the adsorption of I_2 into $[\text{Eu}_2L_3(\text{DMSO})_2(\text{MeOH})_2]$ ($L = 4,4'$ -ethyne-1,2-diyl dibenzoate)^[280] and aromatic molecules into $[\text{Cu}_6L_6]$ (where L is 5,6-diphenyl-1,2,4-triazine-3-thiol)^[281] and $[(\text{ZnCl}_2)_3(\text{tpdpb})]$ (where tpdpb = 1,3,5-tris(*p*-(2,2'-dipyridylamino)phenyl)benzene).^[282] Among a number of systems in which guest molecules coordinate to bare sites on lanthanoid ions and thereby change their luminescent properties,^[283–286] the desorption of bound water from $[\text{Ln}_2(\text{fum})_2(\text{ox})(\text{H}_2\text{O})_4]$ ($\text{Ln} = \text{Eu}, \text{Tb}$; fum = fumarate; ox = oxalate) leads to the almost complete quenching of luminescence, a process that is reversible.^[283] The desorption and subsequent adsorption of ammonia onto the bare Tb^{III} sites within $[\text{Tb}_2(1,4\text{-bdc})_3(\text{H}_2\text{O})_4]$ (MOF-76) leads to a change in the fluorescence decay constants from 1.13 ms^{-1} (H_2O) to 0.74 ms^{-1} (apohost) to 1.00 (NH_3).^[284] The luminescence of its methanol-exchanged analogue, MOF-76b, is enhanced upon exposure to solutions of anions, with fluoride exchange leading to a fourfold increase due to the formation of hydrogen bonding interactions between bound methanol and included anion.^[287] Similar anion sensing capabilities are displayed by $[\text{Tb}^{\text{III}}(\text{mucicate})_{1.5}(\text{H}_2\text{O})_2]$ ^[288] and $[\text{Zn}_2(4,4'\text{-bpy})(\text{H}_2\text{O})_8(\text{ClO}_4)_2(4\text{-aminobenzoate})_2] \cdot 2(4,4'\text{-bpy})$,^[289] with

the latter arising due to replacement of the bound $[\text{ClO}_4]^-$ ions. Cation sensing capabilities have also been exhibited.^[290, 291]

In addition to quenching and enhancement effects, guest-induced shifts in the luminescent emission of the host have been reported. In principle, spectral changes of this type provide a more versatile, albeit potentially less sensitive, approach for molecular sensing than those given above. In $[\text{Zn}_4\text{O}(\text{ntb})_2]$ ($\text{ntb} = 4,4',4''\text{-nitriлотrisbenzoate}$) the presence of host-guest $\pi\text{-}\pi$ interactions leads to a shift in λ_{max} from 435 nm (pyridine) to 456 nm (methanol) to 466 nm (benzene).^[292] The luminescence of this phase likely originates from the ntb linker, although may also result from LMCT within the Zn_4O cluster. A similar behaviour is seen with the adsorption of a range of different guest molecules into $[\text{Zn}_4\text{O}(\text{sdc})_3]$ ($\text{sdc} = \textit{trans}\text{-}4,4'\text{-stilbenedicarboxylate}$).^[293] The absence of any clear relationship between spectral shift and guest polarity for this system suggests that the luminescence is sensitive to the specific nature of the host-guest interaction rather than being determined purely electrostatically.

1.3.3 Structural and Mechanical Properties

In the same way that the subtle energetics associated with guest adsorption and desorption can be sufficient to drive pronounced structural deformations in underconstrained MOF lattices (as described in Section 2.1.2), it has been found that variations in temperature and pressure can also lead to significant structural variation in these systems, both dynamic and static in nature, to yield novel mechanical properties.

1.3.3.1 Anomalous Thermal Expansivities

The expansion of chemical bonds with increasing temperature leads the vast majority of known solids to expand with heating (positive thermal expansion, PTE), a property once thought to be an immutable law of nature. A relatively small number of materials are known that defy this expectation and contract upon heating (*i.e.* display negative thermal expansion, NTE) or are temperature-invariant (*i.e.* display zero thermal expansion, ZTE). These novel behaviours arise due to a range of physical mechanisms that include IVCT,^[294-296] magnetostriction^[297] and, most commonly, transverse lattice vibrations.^[298-300] Examples in the latter class include a family of oxide based materials, the most prominent being ZrW_2O_8 ,^[301] which has a coefficient of thermal expansion $\alpha = d\ell/\ell dT = -9.1 \times 10^{-6} \text{ K}^{-1}$.

Investigation of the thermal expansivities of MOFs has recently led to the discovery of ZTE^[302] and NTE^[303–314] in both cyanide-^[302–311] and benzene(di/tri)carboxylate-bridged frameworks.^[312–314] Structural and theoretical analyses have shown that the multiply hinged molecular linkages of each class confer unprecedented vibrational flexibility to their framework lattices – a feature that is in contrast to all other NTE systems known. In the cyanide phases the double-hinged M-CN-M bridge uniquely allows each metal centre to achieve rotational and translational freedom from its neighbours,^[303] whereas the mechanism for NTE in the polycarboxylate systems is considerably more complex, arising from both local and long-range vibrations.^[312–314]

A direct consequence of the existence of numerous low energy transverse vibrational modes in MOFs is that these materials exhibit extreme NTE behaviours. Among a range of cubic metal cyanide systems that display isotropic NTE,^[303–307] the interpenetrated diamondoid phases Zn(CN)₂ and Cd(CN)₂ have $\alpha = -16.9 \times 10^{-6} \text{ K}^{-1}$ and $-20.4 \times 10^{-6} \text{ K}^{-1}$, respectively.^[303] The desorption of volatile guests from single diamondoid network Cd(CN)₂ to achieve a 64 % porous apohost phase leads to the largest isotropic NTE yet reported for any material, with $\alpha = -33.5 \times 10^{-6} \text{ K}^{-1}$ (see Figure 1.21).^[304] The thermal expansivity of this phase can be tuned by adsorbing guest molecules into the porous framework, as seen for example with N₂ adsorption below 150 K to yield PTE behaviour.

More recently, the generation of noncubic metal cyanide frameworks has led to the discovery of colossal uniaxial NTE in these systems.^[309, 315] In Ag₃[Co(CN)₆], which consists of a 3D lattice of hexagonal symmetry, variation in temperature leads to a highly pronounced temperature-dependent hinging of the structure (see Figure 1.22), resulting in colossal thermal contraction along the *c*-axis ($\alpha_c \cong -125 \times 10^{-6} \text{ K}^{-1}$) and colossal expansion in the *ab*-plane ($\alpha_a \cong +140 \times 10^{-6} \text{ K}^{-1}$).^[309] This property arises due to the very fine balance between the energetics of framework distortion and argentophilic interactions, with the latter favouring increased deformation away from the more regular α -Po (cubic) network geometry with decreasing temperature. Confirmation that the argentophilic interactions play a critical role in this property was provided by analysis of an isostructural Ag-free analogue, H₃[Co(CN)₆], which exhibits conventional expansivities.

1.3.3.2 Compressibilities

Compressibility is an important materials property, both from a fundamental viewpoint in providing information on the energetics of structural deformations, and technologically, with many proposed

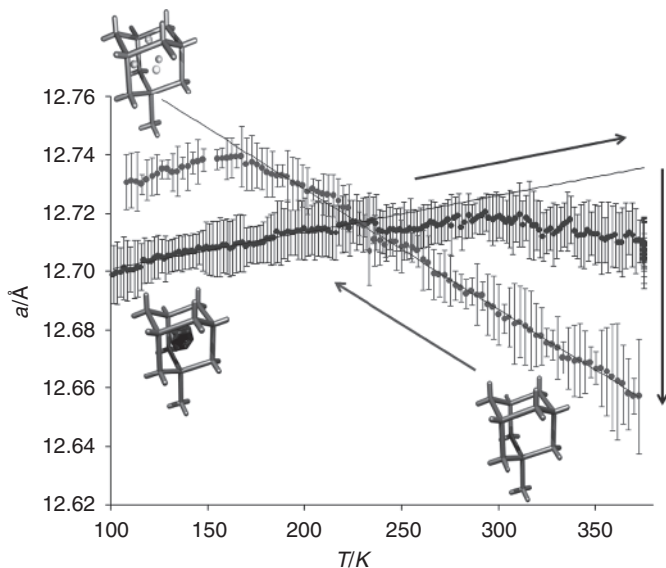


Figure 1.21 Variation in the cubic lattice parameter of $\text{Cd}(\text{CN})_2 \cdot n(\text{guest})$ with temperature. The parent phase $\text{Cd}(\text{CN})_2 \cdot \text{CCl}_4$ displays positive thermal expansion, whereas the apohost $\text{Cd}(\text{CN})_2$ displays the most pronounced isotropic negative thermal expansion behaviour known. Reprinted with permission from A.E. Phillips, A.L. Goodwin, G.J. Halder, P.D. Southon and C.J. Kepert, *Angew. Chem. Int. Ed.*, **47**, 1396. Copyright (2008) Wiley-VCH Verlag GmbH & Co

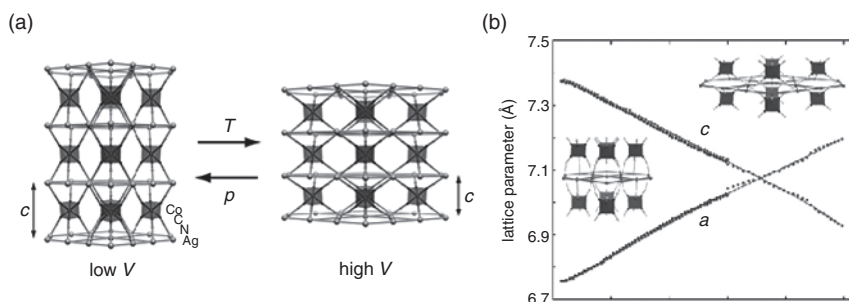


Figure 1.22 (a) Diagrammatic representation of the effect of changes in temperature and isotropic pressure on $\text{Ag}_3[\text{Co}(\text{CN})_6]$. (b) Variation in the a and c parameters of the hexagonal unit cell with temperature, showing the colossal uniaxial NTE along the c -direction. (a) Reprinted with permission from A.L. Goodwin, D.A. Keen and M.G. Tucker, *Proc. Natl. Acad. Sci. USA*, **105**, 18708. Copyright (2008) National Academy of Sciences. (b) Reprinted with permission from A. L. Goodwin, M. Calleja, M. J. Conterio, M. T. Dove, J. S. O. Evans, D. A. Keen, L. Peters, M. G. Tucker, *Science* 2008, **319**, 794–797. Copyright (2008) AAAS

applications for MOFs (*e.g.* in gas separation and storage) requiring sample pelletisation and with pressure potentially representing a useful mechanism for post-synthetic modification of framework structure and adsorption properties. Whereas the compressibilities of materials such as metal oxides have been the subject of considerable investigation, little is currently known about the response of MOFs to external pressures.

Very high compressibilities are expected in MOF lattices due to their relative softness, topological underconstraint and structural openness. A high pressure synchrotron powder X-ray diffraction investigation of $[\text{Cu}_3(\text{btc})_2]$ has confirmed this to be the case, with a bulk modulus [$K = 1/\beta = -V(\partial P/\partial V)_T$ where β is the compressibility] of +30 GPa determined at ambient temperature through the use of nonadsorbing pressure media.^[317] The application of pressure using small-molecule liquids led, in contrast, to interesting behaviours in which the framework was found to be comparatively incompressible at low pressures due to the pressure induced adsorption of the liquids into the pores of the material.

High pressure measurements have also been performed on nonporous MOF phases and novel behaviours observed. The interpenetrated NTE phase $\text{Zn}(\text{CN})_2$ (see Section 1.3.3.1) has $K_0 = 34.2(2)$ GPa and becomes more compressible at higher pressures.^[318] The NTE behaviour of this phase increases at a rate of $-1 \times 10^{-6} \text{ K}^{-1}$ per 0.2 GPa due to a pressure-induced softening of the low energy transverse vibrations. Application of isotropic pressure to the colossal uniaxial NTE phase $\text{Ag}_3[\text{Co}(\text{CN})_6]$ (see Section 1.3.3.1 and Figure 1.22) yields the largest negative linear compressibility (NLC) yet seen for an inorganic material, with $\beta_\ell = -(\partial \ln \ell / \partial P)_T = -76(9) \text{ TPa}^{-1}$ along the *c*-axis.^[316] Positive compressibility is seen in the *ab*-plane, with $\beta_a = 115(8) \text{ TPa}^{-1}$. The bulk modulus for this material is very small [$K = +6.5(3)$ GPa], reflective of very high compressibility.

Lastly, it has been predicted that auxetic properties (*i.e.* negative Poisson ratio; orthogonal contraction upon axial compression, and *vice versa*), which are closely related to NTE, may also arise in MOFs,^[319–321] but this highly sought after behaviour is yet to be reported.

1.4 CONCLUDING REMARKS

The synthesis of MOFs offers enormous scope for the realisation of highly impressive and very useful materials properties. In combining the versatility and diversity of coordination chemistry, organic chemistry and

supramolecular assembly, an unprecedented degree of structural complexity can be incorporated through multiple synthetic steps. The rational design of these materials covers both the identity of the individual building units, with fine chemical control over these being possible prior to, during, and after MOF synthesis, and the way in which they are arranged in space, with an appreciable degree of control over framework structure arising due to the strong directionality of the coordination linkages and to the capacity for post-synthetic modification. Exploitation of the many novel synthetic and structural aspects of these systems has led to the achievement of a diverse range of remarkable chemical and physical properties, many of which are superior to those of all other known classes of material and some of which are unprecedented. Foremost among these has been the achievement of the highest known surface areas for porous materials, leading to unprecedented gravimetric and volumetric uptakes of technologically important gases such as hydrogen and methane, and the generation and stabilisation of the largest known pores within crystalline materials. The fine control over pore structure and surface chemistry has in turn seen the achievement of very high selectivities for guest adsorption, leading to current scale-up efforts for industrially important separation and purification processes. Moreover, the unique ability to generate chiral frameworks through homochiral syntheses rather than chiral surface modification has led to some of the first demonstrations of enantioselective adsorption and heterogeneous catalysis within porous materials. In targeting other advanced forms of physical function, exploitation of the unique magnetic, electronic and optical properties of metal complexes and organic molecules has seen the realisation of a number of remarkable physical properties within porous hosts for the first time. These notably include the generation of porous magnets, porous hosts that are able to switch between multiple spin states, and porous luminescent materials, for each of which the host–guest chemistry and magnetic/electronic/optical functions are intertwined in interesting and potentially useful ways. Investigation of the pronounced structural flexibilities of MOFs has led to the achievement of a range of unprecedented materials properties, both relating to host–guest chemistry and mechanical properties, with the latter notably including the discovery of the highest negative thermal expansivities and nonlinear compressibilities known.

In reflecting on the immensely rich host–guest chemistry of MOFs it is encouraging to note that the numerous achievements highlighted above have emerged almost entirely this century. This extraordinarily rapid development has been made possible by the establishment of many important synthetic design principles in the 1990s and, more generally,

has built on more than 100 years of coordination chemistry research. Given the rapid current expansion of the field, with particular focus both on porosity and on the targeted incorporation of other functional properties, it is reasonable to believe that the broad range of impressive materials properties outlined above are only the tip of the iceberg when considering the future scope for functionality in porous MOFs. In addition to further projected improvements in host–guest properties, considerable scope exists for the combination of multiple properties within individual systems to achieve a diverse array of further unique materials properties, in particular through the control of electron mobility and excitation. Armed with the considerable versatility of coordination chemistry, an ever improving eye for ligand and framework design, and an increasingly sophisticated arsenal of structural and physical characterisation techniques, we can look forward to further rapid developments in the future.

ACKNOWLEDGEMENTS

The author wishes to express his sincere thanks to his students and research fellows, past and present, who have worked tirelessly in MOF chemistry. He is grateful also to the Australian Research Council for providing ARC Discovery and Fellowship Grant funding to study these materials.

REFERENCES

- [1] B.F. Hoskins and R. Robson, *J. Am. Chem. Soc.*, **112**, 1546 (1990).
- [2] J.R. Long and O.M. Yaghi, *Chem. Soc. Rev.*, **38**, 1213 (2009).
- [3] D.J. Tranchemontagne, J.L. Mendoza-Cortes, M. O’Keeffe and O.M. Yaghi, *Chem. Soc. Rev.*, **38**, 1257 (2009).
- [4] M. O’Keeffe, *Chem. Soc. Rev.*, **38**, 1215 (2009).
- [5] S. Kitagawa, R. Kitaura and S. Noro, *Angew. Chem. Int. Ed.*, **43**, 2334 (2004).
- [6] G. Férey, *Chem. Soc. Rev.*, **37**, 191 (2008).
- [7] M.J. Rosseinsky, *Microporous Mesoporous Mater.*, **73**, 15 (2004).
- [8] C.J. Kepert, *Chem. Commun.*, **7**, 695 (2006).
- [9] C.N.R. Rao, A.K. Cheetham and A. Thirumurugan, *J. Phys.: Condens. Matter*, **20**, 083202 (2008).
- [10] C. Janiak, *Dalton Trans.*, **14**, 2781 (2003).
- [11] B. Moulton and M.J. Zaworotko, *Chem. Rev.*, **101**, 1629 (2001).

- [12] R.J. Hill, D.L. Long, N.R. Champness, P. Hubberstey and M. Schröder, *Acc. Chem. Res.*, **38**, 335 (2005).
- [13] D. Maspoch, D. Ruiz-Molina and J. Veciana, *Chem. Soc. Rev.*, **36**, 770 (2007).
- [14] S.L. James, *Chem. Soc. Rev.*, **32**, 276 (2003).
- [15] J.L. Atwood, J.E.D. Davies, D.D. MacNicol and F. Vögtle (Eds), *Comprehensive Supramolecular Chemistry*, Vols 6–10, Pergamon Press, New York, 1996.
- [16] J.L. Atwood, J.E.D. Davies and D.D. MacNicol (Eds), *Inclusion Compounds*, Vols 1–4, Academic Press, London, 1984.
- [17] O.M. Yaghi, G. Li and H. Li, *Nature*, **378**, 703 (1995).
- [18] M. Fujita, J. Yazaki and K. Ogura, *J. Am. Chem. Soc.*, **112**, 5645 (1990).
- [19] R. Robson, *J. Chem. Soc., Dalton Trans.*, 3735 (2000).
- [20] R. Robson, *Dalton Trans.*, 5113 (2008).
- [21] M. Eddaoudi, D.B. Moler, H.L. Li, B.L. Chen, T.M. Reineke, M. O’Keeffe and O.M. Yaghi, *Acc. Chem. Res.*, **34**, 319 (2001).
- [22] O.M. Yaghi, M. O’Keeffe, N.W. Ockwig, H.K. Chae, M. Eddaoudi and J. Kim, *Nature*, **423**, 705 (2003).
- [23] A.F. Wells, *Three-Dimensional Nets and Polyhedra*, Wiley-Interscience, New York, 1977.
- [24] M. O’Keeffe, M.A. Peskov, S.J. Ramsden and O.M. Yaghi, *Acc. Chem. Res.*, **41**, 1782 (2008).
- [25] S. Hyde, O.D. Friedrichs, S.J. Ramsden and V. Robins, *Solid State Sci.*, **8**, 740 (2006).
- [26] L. Ohrström and K. Larsson, *Molecule-Based Materials: The Structural Network Approach*, Elsevier, Amsterdam, 2005.
- [27] S.R. Batten and R. Robson, *Angew. Chem. Int. Ed.*, **37**, 1460 (1998).
- [28] J.J. Perry, J.A. Perman and M.J. Zaworotko, *Chem. Soc. Rev.*, **38**, 1400 (2009).
- [29] J.S. Seo, D. Whang, H. Lee, S.I. Jun, J. Oh, Y.J. Jeon and K. Kim, *Nature*, **404**, 982 (2000).
- [30] R. Vaidhyanathan, D. Bradshaw, J.N. Rebilly, J.P. Barrio, J.A. Gould, N.G. Berry and M.J. Rosseinsky, *Angew. Chem. Int. Ed.*, **45**, 6495 (2006).
- [31] B.F. Abrahams, M. Moylan, S.D. Orchard and R. Robson, *Angew. Chem. Int. Ed.*, **42**, 1848 (2003).
- [32] B. Kesanli and W.B. Lin, *Coord. Chem. Rev.*, **246**, 305 (2003).
- [33] W.B. Lin, *J. Solid State Chem.*, **178**, 2486 (2005).
- [34] D.N. Dybtsev, A.L. Nuzhdin, H. Chun, K.P. Bryliakov, E.P. Talsi, V.P. Fedin and K. Kim, *Angew. Chem. Int. Ed.*, **45**, 916 (2006).
- [35] C.D. Wu, A. Hu, L. Zhang and W.B. Lin, *J. Am. Chem. Soc.*, **127**, 8940 (2005).
- [36] C.D. Wu and W.B. Lin, *Angew. Chem. Int. Ed.*, **46**, 1075 (2007).
- [37] S.S. Iremonger, P.D. Southon and C.J. Kepert, *Dalton Trans.*, 6103 (2008).
- [38] T. Ezuhara, K. Endo and Y. Aoyama, *J. Am. Chem. Soc.*, **121**, 3279 (1999).
- [39] M.J. Ingleson, J.P. Barrio, J. Bacsá, C. Dickinson, H. Park and M.J. Rosseinsky, *Chem. Commun.*, 1287 (2008).
- [40] D. Bradshaw, J.B. Claridge, E.J. Cussen, T.J. Prior and M.J. Rosseinsky, *Acc. Chem. Res.*, **38**, 273 (2005).
- [41] D. Bradshaw, T.J. Prior, E.J. Cussen, J.B. Claridge and M.J. Rosseinsky, *J. Am. Chem. Soc.*, **126**, 6106 (2004).
- [42] C.J. Kepert, T.J. Prior and M.J. Rosseinsky, *J. Am. Chem. Soc.*, **122**, 5158 (2000).
- [43] C.J. Kepert and M.J. Rosseinsky, *Chem. Commun.*, 31 (1998).

- [44] G. Férey and A.K. Cheetham, *Science*, **283**, 1125 (1999).
- [45] G. Férey, C. Mellot-Draznieks, C. Serre and F. Millange, *Acc. Chem. Res.*, **38**, 217 (2005).
- [46] C.T. Kresge, M.E. Leonowicz, W.J. Roth, J.C. Vartuli and J.S. Beck, *Nature*, **359**, 710 (1992).
- [47] Y.K. Park, S.B. Choi, H. Kim, K. Kim, B.H. Won, K. Choi, J.S. Choi, W.S. Ahn, N. Won, S. Kim, D.H. Jung, S.H. Choi, G.H. Kim, S.S. Cha, Y.H. Jhon, J.K. Yang and J. Kim, *Angew. Chem. Int. Ed.*, **46**, 8230 (2007).
- [48] D. Britt, D. Tranchemontagne and O.M. Yaghi, *Proc. Natl. Acad. Sci. U.S.A.*, **105**, 11623 (2008).
- [49] H.K. Chae, D.Y. Siberio-Perez, J. Kim, Y. Go, M. Eddaoudi, A.J. Matzger, M. O’Keeffe and O.M. Yaghi, *Nature*, **427**, 523 (2004).
- [50] H. Li, M. Eddaoudi, M. O’Keeffe and O.M. Yaghi, *Nature*, **402**, 276 (1999).
- [51] M. Eddaoudi, J. Kim, N. Rosi, D. Vodak, J. Wachter, M. O’Keeffe and O.M. Yaghi, *Science*, **295**, 469 (2002).
- [52] G. Férey, C. Mellot-Draznieks, C. Serre, F. Millange, J. Dutour, S. Surblé and I. Margiolaki, *Science*, **309**, 2040 (2005).
- [53] M. Latroche, S. Surble, C. Serre, C. Mellot-Draznieks, P.L. Llewellyn, J.H. Lee, J.S. Chang, S.H. Jhung and G. Férey, *Angew. Chem. Int. Ed.*, **45**, 8227 (2006).
- [54] B. Wang, A.P. Cote, H. Furukawa, M. O’Keeffe and O.M. Yaghi, *Nature*, **453**, 207 (2008).
- [55] K.S. Park, Z. Ni, A.P. Cote, J.Y. Choi, R.D. Huang, F.J. Uribe-Romo, H.K. Chae, M. O’Keeffe and O.M. Yaghi, *Proc. Natl. Acad. Sci. USA*, **103**, 10186 (2006).
- [56] X. Lin, I. Telepeni, A.J. Blake, A. Dailly, C.M. Brown, J.M. Simmons, M. Zoppi, G.S. Walker, K.M. Thomas, T.J. Mays, P. Hubberstey, N.R. Champness and M. Schröder, *J. Am. Chem. Soc.*, **131**, 2159 (2009).
- [57] X. Lin, J.H. Jia, X.B. Zhao, K.M. Thomas, A.J. Blake, G.S. Walker, N.R. Champness, P. Hubberstey and M. Schröder, *Angew. Chem. Int. Ed.*, **45**, 7358 (2006).
- [58] H. Furukawa, M.A. Miller and O.M. Yaghi, *J. Mater. Chem.*, **17**, 3197 (2007).
- [59] Z.Q. Wang and S.M. Cohen, *Chem. Soc. Rev.*, **38**, 1315 (2009).
- [60] J.L.C. Rowsell and O.M. Yaghi, *J. Am. Chem. Soc.*, **128**, 1304 (2006).
- [61] A.P. Nelson, O.K. Farha, K.L. Mulfort and J.T. Hupp, *J. Am. Chem. Soc.*, **131**, 458 (2009).
- [62] S.S.Y. Chui, S.M.F. Lo, J.P.H. Charmant, A.G. Orpen and I.D. Williams, *Science*, **283**, 1148 (1999).
- [63] Y. Liu, G. Li, X. Li and Y. Cui, *Angew. Chem. Int. Ed.*, **46**, 6301 (2007).
- [64] M. Oh and C.A. Mirkin, *Angew. Chem. Int. Ed.*, **45**, 5492 (2006).
- [65] F. Nouar, J. Eckert, J.F. Eubank, P. Forster and M. Eddaoudi, *J. Am. Chem. Soc.*, **131**, 2864 (2009).
- [66] S.R. Halper, L. Do, J.R. Stork and S.M. Cohen, *J. Am. Chem. Soc.*, **128**, 15255 (2006).
- [67] K.S. Min and M.P. Suh, *J. Am. Chem. Soc.*, **122**, 6834 (2000).
- [68] S. Das, H. Kim and K. Kim, *J. Am. Chem. Soc.*, **131**, 3814 (2009).
- [69] S. Bureekaew, S. Horike, M. Higuchi, M. Mizuno, T. Kawamura, D. Tanaka, N. Yanai and S. Kitagawa, *Nat. Mater.*, **8**, 831 (2009).
- [70] H. Kitagawa, Y. Nagao, M. Fujishima, R. Ikeda and S. Kanda, *Inorg. Chem. Commun.*, **6**, 346 (2003).
- [71] L.Q. Ma, C. Abney and W.B. Lin, *Chem. Soc. Rev.*, **38**, 1248 (2009).

- [72] Y.K. Hwang, D.Y. Hong, J.S. Chang, S.H. Jhung, Y.K. Seo, J. Kim, A. Vimont, M. Daturi, C. Serre and G. Férey, *Angew. Chem. Int. Ed.*, **47**, 4144 (2008).
- [73] S.S. Kaye and J.R. Long, *J. Am. Chem. Soc.*, **130**, 806 (2008).
- [74] H.J. Choi and M.P. Suh, *J. Am. Chem. Soc.*, **126**, 15844 (2004).
- [75] K.L. Mulfort and J.T. Hupp, *Inorg. Chem.*, **47**, 7936 (2008).
- [76] K.L. Mulfort, T.M. Wilson, M.R. Wasielewski and J.T. Hupp, *Langmuir*, **25**, 503 (2009).
- [77] K.K. Tanabe, Z.Q. Wang and S.M. Cohen, *J. Am. Chem. Soc.*, **130**, 8508 (2008).
- [78] M.J. Ingleson, J.P. Barrio, J.B. Guilbaud, Y.Z. Khimiyak and M.J. Rosseinsky, *Chem. Commun.*, 2680 (2008).
- [79] G.J. Halder and C.J. Kepert, *J. Am. Chem. Soc.*, **127**, 7891 (2005).
- [80] R. Kitaura, S. Kitagawa, Y. Kubota, T.C. Kobayashi, K. Kindo, Y. Mita, A. Matsuo, M. Kobayashi, H.C. Chang, T.C. Ozawa, M. Suzuki, M. Sakata and M. Takata, *Science*, **298**, 2358 (2002).
- [81] P.V. Ganesan and C.J. Kepert, *Chem. Commun.*, 2168 (2004).
- [82] C.J. Kepert and M.J. Rosseinsky, *Chem. Commun.*, 375 (1999).
- [83] B.F. Abrahams, P.A. Jackson and R. Robson, *Angew. Chem. Int. Ed.*, **37**, 2656 (1998).
- [84] B. Rather and M.J. Zaworotko, *Chem. Commun.*, 830 (2003).
- [85] E.Y. Lee and M.P. Suh, *Angew. Chem. Int. Ed.*, **43**, 2798 (2004).
- [86] K. Biradha, Y. Hongo and M. Fujita, *Angew. Chem. Int. Ed.*, **39**, 3843 (2000).
- [87] A.J. Fletcher, E.J. Cussen, T.J. Prior, M.J. Rosseinsky, C.J. Kepert and K.M. Thomas, *J. Am. Chem. Soc.*, **123**, 10001 (2001).
- [88] M. Kondo, M. Shimamura, S.-Noro, S. Minakoshi, A. Asami, K. Seki and S. Kitagawa, *Chem. Mater.*, **12**, 1288 (2000).
- [89] M. Kondo, T. Yoshitomi, K. Seki, H. Matsuzaka and S. Kitagawa, *Angew. Chem. Int. Ed.*, **36**, 1725 (1997).
- [90] H. Li, M. Eddaoudi, T.L. Groy and O.M. Yaghi, *J. Am. Chem. Soc.*, **120**, 8571 (1998).
- [91] T. Duren, Y.S. Bae and R.Q. Snurr, *Chem. Soc. Rev.*, **38**, 1237 (2009).
- [92] S.S. Han, J.L. Mendoza-Cortes and W.A. Goddard, *Chem. Soc. Rev.*, **38**, 1460 (2009).
- [93] E.J. Cussen, J.B. Claridge, M.J. Rosseinsky and C.J. Kepert, *J. Am. Chem. Soc.*, **124**, 9574 (2002).
- [94] M.P. Suh, J.W. Ko and H.J. Choi, *J. Am. Chem. Soc.*, **124**, 10976 (2002).
- [95] K. Biradha and M. Fujita, *Angew. Chem. Int. Ed.*, **41**, 3392 (2002).
- [96] H. Kumagai, K.W. Chapman, C.J. Kepert and M. Kurmoo, *Polyhedron*, **22**, 1921 (2003).
- [97] G.J. Halder, C.J. Kepert, B. Moubaraki, K.S. Murray and J.D. Cashion, *Science*, **298**, 1762 (2002).
- [98] R. Kitaura, K. Fujimoto, S. Noro, M. Kondo and S. Kitagawa, *Angew. Chem. Int. Ed.*, **41**, 133 (2002).
- [99] G. Férey and C. Serre, *Chem. Soc. Rev.*, **38**, 1380 (2009).
- [100] R. Kitaura, K. Seki, G. Akiyama and S. Kitagawa, *Angew. Chem. Int. Ed.*, **42**, 428 (2003).
- [101] A.J. Fletcher, E.J. Cussen, T.J. Prior, M.J. Rosseinsky, C.J. Kepert and K.M. Thomas, *J. Am. Chem. Soc.*, **123**, 10001 (2001).
- [102] F. Millange, C. Serre, N. Guillou, G. Férey and R.I. Walton, *Angew. Chem. Int. Ed.*, **47**, 4100 (2008).

- [103] Y. Liu, J.H. Her, A. Dailly, A.J. Ramirez-Cuesta, D.A. Neumann and C.M. Brown, *J. Am. Chem. Soc.*, **130**, 11813 (2008).
- [104] S. Bourrelly, P.L. Llewellyn, C. Serre, F. Millange, T. Loiseau and G. Férey, *J. Am. Chem. Soc.*, **127**, 13519 (2005).
- [105] A. Pichon, A. Lazuen-Garay and S.L. James, *CrystEngComm*, **8**, 211 (2006).
- [106] V. Niel, A.L. Thompson, M.C. Muñoz, A. Galet, A.S.E. Goeta and J.A. Real, *Angew. Chem. Int. Ed.*, **42**, 3760 (2003).
- [107] A.V. Nossorov, D.V. Soldatov and J.A. Ripmeester, *J. Am. Chem. Soc.*, **123**, 3563 (2001).
- [108] M. Edgar, R. Mitchell, A.M.Z. Slawin, P. Lightfoot and P.A. Wright, *Chem. Eur. J.*, **7**, 5168 (2001).
- [109] J.J. Vittal, *Coord. Chem. Rev.*, **251**, 1781 (2007).
- [110] G.S. Papaefstathiou, Z. Zhong, L. Geng and L.R. MacGillivray, *J. Am. Chem. Soc.*, **126**, 9158 (2004).
- [111] G.S. Papaefstathiou, I.G. Georgiev, T. Friscic and L.R. MacGillivray, *Chem. Commun.*, 3974 (2005).
- [112] N.L. Toh, M. Nagarathinam and J.J. Vittal, *Angew. Chem. Int. Ed.*, **44**, 2237 (2005).
- [113] M.J. Vela, B.B. Snider and B.M. Foxman, *Chem. Mater.*, **10**, 3167 (1998).
- [114] T. Uemura, N. Yanai and S. Kitagawa, *Chem. Soc. Rev.*, **38**, 1228 (2009).
- [115] R.E. Morris and P.S. Wheatley, *Angew. Chem. Int. Ed.*, **47**, 4966 (2008).
- [116] L.J. Murray, M. Dincă and J.R. Long, *Chem. Soc. Rev.*, **38**, 1294 (2009).
- [117] K.M. Thomas, *Dalton Trans.*, 1487 (2009).
- [118] J.L.C. Rowsell and O.M. Yaghi, *Angew. Chem. Int. Ed.*, **44**, 4670 (2005).
- [119] D.J. Collins and H.C. Zhou, *J. Mater. Chem.*, **17**, 3154 (2007).
- [120] H. Wu, W. Zhou and T. Yildirim, *J. Am. Chem. Soc.*, **131**, 4995 (2009).
- [121] R. Matsuda, R. Kitaura, S. Kitagawa, Y. Kubota, R.V. Belosludov, T.C. Kobayashi, H. Sakamoto, T. Chiba, M. Takata, Y. Kawazoe and Y. Mita, *Nature*, **436**, 238 (2005).
- [122] S.C. Xiang, W. Zhou, J.M. Gallegos, Y. Liu and B.L. Chen, *J. Am. Chem. Soc.*, **131**, 12415 (2009).
- [123] P. Horcajada, C. Serre, G. Maurin, N.A. Ramsahye, F. Balas, M. Vallet-Regi, M. Sebban, F. Taulelle and G. Férey, *J. Am. Chem. Soc.*, **130**, 6774 (2008).
- [124] P. Horcajada, C. Serre, M. Vallet-Regi, M. Sebban, F. Taulelle and G. Férey, *Angew. Chem. Int. Ed.*, **45**, 5974 (2006).
- [125] W.J. Rieter, K.M. Pott, K.M.L. Taylor and W.B. Lin, *J. Am. Chem. Soc.*, **130**, 11584 (2008).
- [126] J.L.C. Rowsell, A.R. Millward, K.S. Park and O.M. Yaghi, *J. Am. Chem. Soc.*, **126**, 5666 (2004).
- [127] S.S. Kaye, A. Dailly, O.M. Yaghi and J.R. Long, *J. Am. Chem. Soc.*, **129**, 14176 (2007).
- [128] A.G. Wong-Foy, A.J. Matzger and O.M. Yaghi, *J. Am. Chem. Soc.*, **128**, 3494 (2006).
- [129] M. Dincă, A. Dailly, Y. Liu, C.M. Brown, D.A. Neumann and J.R. Long, *J. Am. Chem. Soc.*, **128**, 16876 (2006).
- [130] V.K. Peterson, Y. Liu, C.M. Brown and C.J. Kepert, *J. Am. Chem. Soc.*, **128**, 15578 (2006).
- [131] P.M. Forster, J. Eckert, B.D. Heiken, J.B. Parise, J.W. Yoon, S.H. Jhung, J.S. Chang and A.K. Cheetham, *J. Am. Chem. Soc.*, **128**, 16846 (2006).

- [132] S.S. Kaye and J.R. Long, *Chem. Commun.*, 4486 (2007).
- [133] J.G. Vitillo, L. Regli, S. Chavan, G. Ricchiardi, G. Spoto, P.D.C. Dietzel, S. Bordiga and A. Zecchina, *J. Am. Chem. Soc.*, **130**, 8386 (2008).
- [134] B. Chen, X. Zhao, A. Putkham, K. Hong, E.B. Lobkovsky, E.J. Hurtado, A.J. Fletcher and K.M. Thomas, *J. Am. Chem. Soc.*, **130**, 6411 (2008).
- [135] X.B. Zhao, B. Xiao, A.J. Fletcher, K.M. Thomas, D. Bradshaw and M.J. Rosseinsky, *Science*, **306**, 1012 (2004).
- [136] J.R. Li, R.J. Kuppler and H.C. Zhou, *Chem. Soc. Rev.*, **38**, 1477 (2009).
- [137] C. Radu and A.M. Bruce, *Eur. J. Inorg. Chem.*, **2007**, 1321 (2007).
- [138] S. Ahuja, In *Chiral Separations: An Overview*, Vol. **471**, S. Ahuja (Ed), American Chemical Society, Washington, DC, 1991, p. 1.
- [139] S. Allenmark, *Chromatographic Enantioseparations*, Ellis Horwood, New York, 1991.
- [140] D.N. Dybtsev, H. Chun, S.H. Yoon, D. Kim and K. Kim, *J. Am. Chem. Soc.*, **126**, 32 (2004).
- [141] M. Dincă and J.R. Long, *J. Am. Chem. Soc.*, **127**, 9376 (2005).
- [142] H.R. Li, Y. Tao, Q. Yu, X.H. Bu, H. Sakamoto and S. Kitagawa, *Chem. Eur. J.*, **14**, 2771 (2008).
- [143] S.Q. Ma, X.S. Wang, C.D. Collier, E.S. Manis and H.C. Zhou, *Inorg. Chem.*, **46**, 8499 (2007).
- [144] R. Banerjee, A. Phan, B. Wang, C. Knobler, H. Furukawa, M. O’Keeffe and O.M. Yaghi, *Science*, **319**, 939 (2008).
- [145] H.L. Guo, G.S. Zhu, I.J. Hewitt and S.L. Qiu, *J. Am. Chem. Soc.*, **131**, 1646 (2009).
- [146] T.K. Maji, K. Uemura, H.C. Chang, R. Matsuda and S. Kitagawa, *Angew. Chem. Int. Ed.*, **43**, 3269 (2004).
- [147] S.Q. Ma, D.F. Sun, X.S. Wang and H.C. Zhou, *Angew. Chem. Int. Ed.*, **46**, 2458 (2007).
- [148] H.M. Powell and J.H. Rayner, *Nature*, **163**, 566 (1949).
- [149] T. Iwamoto, in *Inclusion Compounds I*, J.L. Atwood, J.E.D. Davies and D.D. MacNicol (Eds), Academic Press, London, 1984, p. 29.
- [150] J.S. Seo, D. Whang, H. Lee, S.I. Jun, J. Oh, Y.J. Jeon and K. Kim, *Nature*, **404**, 982 (2000).
- [151] O.R. Evans, H.L. Ngo and W.B. Lin, *J. Am. Chem. Soc.*, **123**, 10395 (2001).
- [152] Y. Cui, O.R. Evans, H.L. Ngo, P.S. White and W.B. Lin, *Angew. Chem. Int. Ed.*, **41**, 1159 (2002).
- [153] Y. Cui, S.J. Lee and W.B. Lin, *J. Am. Chem. Soc.*, **125**, 6014 (2003).
- [154] Y. Cui, H.L. Ngo, P.S. White and W.B. Lin, *Inorg. Chem.*, **42**, 652 (2003).
- [155] R.G. Xiong, X.Z. You, B.F. Abrahams, Z.L. Xue and C.M. Che, *Angew. Chem. Int. Ed.*, **40**, 4422 (2001).
- [156] M. Fujita, Y.J. Kwon, S. Washizu and K. Ogura, *J. Am. Chem. Soc.*, **116**, 1151 (1994).
- [157] J. Lee, O.K. Farha, J. Roberts, K.A. Scheidt, S.T. Nguyen and J.T. Hupp, *Chem. Soc. Rev.*, **38**, 1450 (2009).
- [158] A.U. Czaja, N. Trukhan and U. Müller, *Chem. Soc. Rev.*, **38**, 1284 (2009).
- [159] S. Kitagawa, S. Noro and T. Nakamura, *Chem. Commun.*, 701 (2006).
- [160] L. Alaerts, E. Seguin, H. Poelman, F. Thibault-Starzyk, P.A. Jacobs and D.E. DeVos, *Chem. Eur. J.*, **12**, 7353 (2006).

- [161] K. Schlichte, T. Kratzke and S. Kaskel, *Microporous Mesoporous Mater.*, **73**, 81 (2004).
- [162] A. Henschel, K. Gedrich, R. Kraehnert and S. Kaskel, *Chem. Commun.*, 4192 (2008).
- [163] S. Horike, M. Dincă, K. Tamaki and J.R. Long, *J. Am. Chem. Soc.*, **130**, 5854 (2008).
- [164] S.H. Cho, B.Q. Ma, S.T. Nguyen, J.T. Hupp and T.E. Albrecht-Schmitt, *Chem. Commun.*, 2563 (2006).
- [165] M.H. Alkordi, Y.L. Liu, R.W. Larsen, J.F. Eubank and M. Eddaoudi, *J. Am. Chem. Soc.*, **130**, 12639 (2008).
- [166] S. Hermis, M.K. Schroter, R. Schmid, L. Khodeir, M. Muhler, A. Tissler, R.W. Fischer and R.A. Fischer, *Angew. Chem. Int. Ed.*, **44**, 6237 (2005).
- [167] O. Kahn, *Molecular Magnetism*, VCH, New York, 1993.
- [168] R.L. Carlin and A.J. van Duynveldt, *Magnetic Properties of Transition Metal Compounds*, Vol. 2, Springer-Verlag, New York, 1977.
- [169] R.L. Carlin, *Magnetochemistry*, Springer-Verlag, Berlin, 1986.
- [170] H.O. Stumpf, L. Ouahab, Y. Pei, D. Grandjean and O. Kahn, *Science*, **261**, 447 (1993).
- [171] X.Y. Wang, Z.M. Wang and S. Gao, *Chem. Commun.*, 281 (2008).
- [172] M. Kurmoo, *Chem. Soc. Rev.*, **38**, 1353 (2009).
- [173] S. Decurtins, H.W. Schmalle, P. Schnewly, J. Ensling and P. Gütlich, *J. Am. Chem. Soc.*, **116**, 9521 (1994).
- [174] S.G. Carling, C. Mathoniere, P. Day, K.M.A. Malik, S.J. Coles and M.B. Hursthouse, *J. Chem. Soc., Dalton Trans.*, 1839 (1996).
- [175] H.Z. Kou and O. Sato, *Inorg. Chem.*, **46**, 9513 (2007).
- [176] X.Y. Wang, L. Gan, S.W. Zhang and S. Gao, *Inorg. Chem.*, **43**, 4615 (2004).
- [177] Z.M. Wang, B. Zhang, T. Otsuka, K. Inoue, H. Kobayashi and M. Kurmoo, *Dalton Trans.*, 2209 (2004).
- [178] O. Kahn, J. Larionova and J.V. Yakhmi, *Chem. Eur. J.*, **5**, 3443 (1999).
- [179] A. Rujiwatra, C.J. Kepert and M.J. Rosseinsky, *Chem. Commun.*, 2307 (1999).
- [180] A. Rujiwatra, C.J. Kepert, J.B. Claridge, M.J. Rosseinsky, H. Kumagai and M. Kurmoo, *J. Am. Chem. Soc.*, **123**, 10584 (2001).
- [181] M. Kurmoo, H. Kumagai, S.M. Hughes and C.J. Kepert, *Inorg. Chem.*, **42**, 6709 (2003).
- [182] D. Maspoch, D. Ruiz-Molina, K. Wurst, N. Domingo, M. Cavallini, F. Biscarini, J. Tejada, C. Rovira and J. Veciana, *Nat. Mater.*, **2**, 190 (2003).
- [183] M. Kurmoo, H. Kumagai, K.W. Chapman and C.J. Kepert, *Chem. Commun.*, 3012 (2005).
- [184] S.S. Kaye, H.J. Choi and J.R. Long, *J. Am. Chem. Soc.*, **130**, 16921 (2008).
- [185] X.-M. Zhang, Z.-M. Hao, W.-X. Zhang and X.-M. Chen, *Angew. Chem. Int. Ed.*, **46**, 3456 (2007).
- [186] S. Xiang, X. Wu, J. Zhang, R. Fu, S. Hu and X. Zhang, *J. Am. Chem. Soc.*, **127**, 16352 (2005).
- [187] R.D. Poulsen, A. Bentien, M. Chevalier and B.B. Iversen, *J. Am. Chem. Soc.*, **127**, 9156 (2005).
- [188] Z. Wang, X. Zhang, S.R. Batten, M. Kurmoo and S. Gao, *Inorg. Chem.*, **46**, 8439 (2007).
- [189] R. Kuhlman, G.L. Schimek and J.W. Kolis, *Inorg. Chem.*, **38**, 194 (1999).

- [190] S.O.H. Gutschke, D.J. Price, A.K. Powell and P.T. Wood, *Angew. Chem. Int. Ed.*, **38**, 1088 (1999).
- [191] M. Kurmoo, H. Kumagai, K.W. Chapman and C.J. Kepert, *Chem. Commun.*, 3012 (2005).
- [192] M. Kurmoo, H. Kumagai, M. Akita-Tanaka, K. Inoue and S. Takagi, *Inorg. Chem.*, **45**, 1627 (2006).
- [193] K. Barthelet, J. Marrot, D. Riou and G. Férey, *Angew. Chem. Int. Ed.*, **41**, 281 (2002).
- [194] C. Serre, F. Millange, C. Thouvenot, M. Nogues, G. Marsolier, D. Louer and G. Férey, *J. Am. Chem. Soc.*, **124**, 13519 (2002).
- [195] M. Kurmoo, H. Kumagai, S.M. Hughes and C.J. Kepert, *Inorg. Chem.*, **42**, 6709 (2003).
- [196] M. Riou-Cavellec, C. Albinet, C. Livage, N. Guillou, M. Noguès, J.M. Grenèche and G. Férey, *Solid State Sci.*, **4**, 267 (2002).
- [197] M. Viertelhaus, H. Henke, C.E. Anson and A.K. Powell, *Eur. J. Inorg. Chem.*, 2283 (2003).
- [198] Z. Wang, B. Zhang, H. Fujiwara, H. Kobayashi and M. Kurmoo, *Chem. Commun.*, 416 (2004).
- [199] Z. Wang, B. Zhang, M. Kurmoo, M.A. Green, H. Fujiwara, T. Otsuka and H. Kobayashi, *Inorg. Chem.*, **44**, 1230 (2005).
- [200] Z. Wang, Y. Zhang, M. Kurmoo, T. Liu, S. Vilminot, B. Zhao and S. Gao, *Aust. J. Chem.*, **59**, 617 (2006).
- [201] Z. Wang, B. Zhang, Y. Zhang, M. Kurmoo, T. Liu, S. Gao and H. Kobayashi, *Polyhedron*, **26**, 2207 (2007).
- [202] Z. Wang, Y. Zhang, T. Liu, M. Kurmoo and S. Gao, *Adv. Funct. Mater.*, **17**, 1523 (2007).
- [203] B. Zhang, Z. Wang, M. Kurmoo, S. Gao, K. Inoue and H. Kobayashi, *Adv. Funct. Mater.*, **17**, 577 (2007).
- [204] K.R. Dunbar and R.A. Heintz, in *Progress in Inorganic Chemistry*, Vol. 45, John Wiley & Sons Inc., New York, 1997, p. 283.
- [205] M. Verdagner, A. Bleuzen, V. Marvaud, J. Vaissermann, M. Seuleiman, C. Desplanches, A. Sculler, C. Train, R. Garde, G. Gelly, C. Lomenech, I. Rosenman, P. Veillet, C. Cartier and F. Villain, *Coord. Chem. Rev.*, **192**, 1023 (1999).
- [206] M. Verdagner, A. Bleuzen, C. Train, R. Garde, F.F. de Biani and C. Desplanches, *Philos. Trans. R. Soc. London, Ser. A*, **357**, 2959 (1999).
- [207] D. Davidson and L.A. Welo, *J. Phys. Chem.*, **32**, 1191 (1928).
- [208] V. Gadet, T. Mallah, I. Castro and M. Verdagner, *J. Am. Chem. Soc.*, **114**, 9213 (1992).
- [209] T. Mallah, S. Thiebaut, M. Verdagner and P. Veillet, *Science*, **262**, 1554 (1993).
- [210] S. Ferlay, T. Mallah, R. Ouahes, P. Veillet and M. Verdagner, *Nature*, **378**, 701 (1995).
- [211] Ø. Hatlevik, W.E. Buschmann, J. Zhang, J.L. Manson and J.S. Miller, *Adv. Mater.*, **11**, 914 (1999).
- [212] S.M. Holmes and G.S. Girolami, *J. Am. Chem. Soc.*, **121**, 5593 (1999).
- [213] M. Ohba and H. Ōkawa, *Coord. Chem. Rev.*, **198**, 313 (2000).
- [214] M. Ohba, N. Maruono, H. Ōkawa, T. Enoki and J.M. Latour, *J. Am. Chem. Soc.*, **116**, 11566 (1994).
- [215] M. Ohba, N. Usuki, N. Fukita and H. Ōkawa, *Angew. Chem. Int. Ed.*, **38**, 1795 (1999).

- [216] G. Boxhoorn, J. Moolhuysen, J.G.F. Coolegem and R.A. van Santen, *J. Chem. Soc., Chem. Commun.*, 1305 (1985).
- [217] S.S. Kaye and J.R. Long, *J. Am. Chem. Soc.*, **127**, 6506 (2005).
- [218] K.W. Chapman, P.D. Southon, C.L. Weeks and C.J. Kepert, *Chem. Commun.*, 3322 (2005).
- [219] K.W. Chapman, P.J. Chupas and C.J. Kepert, *J. Am. Chem. Soc.*, **127**, 11232 (2005).
- [220] Y. Sato, S. Ohkoshi, K. Arai, M. Tozawa and K. Hashimoto, *J. Am. Chem. Soc.*, **125**, 14590 (2003).
- [221] S. Ohkoshi, K.I. Arai, Y. Sato and K. Hashimoto, *Nat. Mat.*, **3**, 857 (2004).
- [222] Z. Lu, X. Wang, Z. Liu, F. Liao, S. Gao, R. Xiong, H. Ma, D. Zhang and D. Zhu, *Inorg. Chem.*, **45**, 999 (2006).
- [223] W. Kaneko, M. Ohba and S. Kitagawa, *J. Am. Chem. Soc.*, **129**, 13706 (2007).
- [224] B. Nowicka, M. Rams, K. Stadnicka and B. Sieklucka, *Inorg. Chem.*, **46**, 8123 (2007).
- [225] S. Ohkoshi, Y. Tsunobuchi, H. Takahashi, T. Hozumi, M. Shiro and K. Hashimoto, *J. Am. Chem. Soc.*, **129**, 3084 (2007).
- [226] W. Kaim and M. Moscherosch, *Coord. Chem. Rev.*, **129**, 157 (1994).
- [227] J.-H. Her, P.W. Stephens, K.I. Pokhodnya, M. Bonner and J.S. Miller, *Angew. Chem. Int. Ed.*, **46**, 1521 (2007).
- [228] K.I. Pokhodnya, M. Bonner, J.-H. Her, P.W. Stephens and J.S. Miller, *J. Am. Chem. Soc.*, **128**, 15592 (2006).
- [229] H. Miyasaka, T. Izawa, N. Takahashi, M. Yamashita and K.R. Dunbar, *J. Am. Chem. Soc.*, **128**, 11358 (2006).
- [230] N. Motokawa, H. Miyasaka, M. Yamashita and K.R. Dunbar, *Angew. Chem. Int. Ed.*, **47**, 7760 (2008).
- [231] S. Shimomura, R. Matsuda, T. Tsujino, T. Kawamura and S. Kitagawa, *J. Am. Chem. Soc.*, **128**, 16416 (2006).
- [232] D. Maspoch, N. Domingo, D.R. Molina, K. Wurst, J.M. Hernandez, G. Vaughan, C. Rovira, F. Lloret, J. Tejada and J. Veciana, *Chem. Commun.*, 5035 (2005).
- [233] D. Maspoch, D. Ruiz-Molina, K. Wurst, C. Rovira and J. Veciana, *Chem. Commun.*, 1164 (2004).
- [234] P. Gütllich, A. Hauser and H. Spiering, *Angew. Chem. Int. Ed.*, **33**, 2024 (1994).
- [235] O. Kahn and C.J. Martinez, *Science*, **279**, 44 (1998).
- [236] Y. Garcia, P.J. van Koningsbruggen, R. Lapouyade, L. Fournes, L. Rabardel, O. Kahn, V. Ksenofontov, G. Levchenko and P. Gütllich, *Chem. Mater.*, **10**, 2426 (1998).
- [237] J.G. Haasnoot, *Coord. Chem. Rev.*, **200**, 131 (2000).
- [238] L.G. Lavrenova, N.G. Yudina, V.N. Ikorskii, V.A. Varnek, I.M. Oglezneva and S.V. Larionov, *Polyhedron*, **14**, 1333 (1995).
- [239] J.A. Real, E. Andres, M.C. Muñoz, M. Julve, T. Granier, A. Bousseksou and F. Varret, *Science*, **268**, 265 (1995).
- [240] V. Niel, J.M. Martinez-Agudo, M.C. Muñoz, A.B. Gaspar and J.A. Real, *Inorg. Chem.*, **40**, 3838 (2001).
- [241] P. Gütllich, Y. Garcia and H.A. Goodwin, *Chem. Soc. Rev.*, **29**, 419 (2000).
- [242] Y. Garcia, P.J. van Koningsbruggen, R. Lapouyade, L. Rabardel, O. Kahn, M. Wiczcerek, R. Bronisz, Z. Ciunik and M.F. Rudolf, *C. R. Acad. Sci.*, **1**, 523 (1998).

- [243] W. Vreugdenhil, J.H. van Diemen, R.A.G. de Graaff, J.G. Haasnoot, J. Reedijk, A.M. van der Kraan, O. Kahn and J. Zarembowitch, *Polyhedron*, **9**, 2971 (1990).
- [244] Y. Garcia, O. Kahn, L. Rabardel, C. Benoit, L. Salmon and J.P. Tuchagues, *Inorg. Chem.*, **38**, 4663 (1999).
- [245] P.J. van Koningsbruggen, Y. Garcia, G. Bravic, D. Chasseau and O. Kahn, *Inorg. Chim. Acta*, **326**, 101 (2001).
- [246] J.A. Real, A.B. Gaspar, V. Niel and M.C. Muñoz, *Coord. Chem. Rev.*, **236**, 121 (2003).
- [247] P.J. van Koningsbruggen, Y. Garcia, O. Kahn, L. Fournes, H. Kooijman, A.L. Spek, J.G. Haasnoot, J. Moscovici, K. Provost, A. Michalowicz, F. Renz and P. Gütllich, *Inorg. Chem.*, **39**, 1891 (2000).
- [248] C.M. Grunert, J. Schweifer, P. Weinberger, W. Linert, K. Mereiter, G. Hilscher, M. Muller, G. Wiesinger and P.J. van Koningsbruggen, *Inorg. Chem.*, **43**, 155 (2004).
- [249] T. Kitazawa, Y. Gomi, M. Takahashi, M. Takeda, M. Enomoto, A. Miyazaki and T. Enoki, *J. Mater. Chem.*, **6**, 119 (1996).
- [250] W. Kosaka, K. Nomura, K. Hashimoto and S. Ohkoshi, *J. Am. Chem. Soc.*, **127**, 8590 (2005).
- [251] D. Papanikolaou, S. Margadonna, W. Kosaka, S. Ohkoshi, M. Brunelli and K. Prassides, *J. Am. Chem. Soc.*, **128**, 8358 (2006).
- [252] K.S. Murray and C.J. Kepert, in *Topics in Current Chemistry*, Vol. 233, P. Gütllich and H.A. Goodwin (Eds), Springer-Verlag, Heidelberg, 2004, p. 195.
- [253] G.J. Halder, K.W. Chapman, S.M. Neville, B. Moubaraki, K.S. Murray, J.F. Létard and C.J. Kepert, *J. Am. Chem. Soc.*, **130**, 17552 (2008).
- [254] S.M. Neville, G.J. Halder, K.W. Chapman, M.B. Duriska, P.D. Southon, J.D. Cashion, J.-F. Létard, B. Moubaraki, K.S. Murray and C.J. Kepert, *J. Am. Chem. Soc.*, **130**, 2869 (2008).
- [255] S.M. Neville, B. Moubaraki, K.S. Murray and C.J. Kepert, *Angew. Chem. Int. Ed.*, **46**, 2059 (2007).
- [256] S.M. Neville, G.J. Halder, K.W. Chapman, M.B. Duriska, B. Moubaraki, K.S. Murray and C.J. Kepert, *J. Am. Chem. Soc.*, **131**, 12106 (2009).
- [257] S. Bonhommeau, G. Molnar, A. Galet, A. Zwick, J.A. Real, J.J. McGarvey and A. Bousseksou, *Angew. Chem. Int. Ed.*, **44**, 4069 (2005).
- [258] P.D. Southon, L. Liu, E.A. Fellows, D.J. Price, G.J. Halder, K.W. Chapman, B. Moubaraki, K.S. Murray, J.F. Létard and C.J. Kepert, *J. Am. Chem. Soc.*, **131**, 10998 (2009).
- [259] M. Ohba, K. Yoneda, G. Agusti, M.C. Muñoz, A.B. Gaspar, J.A. Real, M. Yamasaki, H. Ando, Y. Nakao, S. Sakaki and S. Kitagawa, *Angew. Chem. Int. Ed.*, **48**, 4767 (2009).
- [260] P. Day, N.S. Hush and R.J.H. Clark, *Philos. Trans. R. Soc. London, Ser. A*, **366**, 5 (2008).
- [261] O. Sato, T. Iyoda, A. Fujishima and K. Hashimoto, *Science*, **272**, 704 (1996).
- [262] O. Sato, Y. Einaga, A. Fujishima and K. Hashimoto, *Inorg. Chem.*, **38**, 4405 (1999).
- [263] H. Tokoro, T. Matsuda, T. Nuida, Y. Moritomo, K. Ohoyama, E.D.L. Dangui, K. Boukheddaden and S. Ohkoshi, *Chem. Mater.*, **20**, 423 (2008).
- [264] H. Tokoro, S. Ohkoshi and K. Hashimoto, *Appl. Phys. Lett.*, **82**, 1245 (2003).
- [265] S. Ohkoshi and K. Hashimoto, *J. Am. Chem. Soc.*, **121**, 10591 (1999).
- [266] S. Ohkoshi, H. Tokoro, T. Hozumi, Y. Zhang, K. Hashimoto, C. Mathoniere, I. Bord, G. Rombaut, M. Verelst, C.C.D. Moulin and F. Villain, *J. Am. Chem. Soc.*, **128**, 270 (2006).

- [267] Y. Arimoto, S. Ohkoshi, Z.J. Zhong, H. Seino, Y. Mizobe and K. Hashimoto, *J. Am. Chem. Soc.*, **125**, 9240 (2003).
- [268] S. Ohkoshi, S. Ikeda, T. Hozumi, T. Kashiwagi and K. Hashimoto, *J. Am. Chem. Soc.*, **128**, 5320 (2006).
- [269] D.N. Hendrickson and C.G. Pierpont, in *Spin Crossover in Transition Metal Compounds II, Topics in Current Chemistry*, Vol. **234**, P. Gütllich and H.A. Goodwin (Eds), Springer-Verlag, Berlin, 2004, p. 63.
- [270] D.M. Adams, A. Dei, A.L. Rheingold and D.N. Hendrickson, *Angew. Chem. Int. Ed.*, **32**, 880 (1993).
- [271] O.S. Jung and C.G. Pierpont, *J. Am. Chem. Soc.*, **116**, 2229 (1994).
- [272] C.W. Lange, M. Foldeaki, V.I. Nevodchikov, V.K. Cherkasov, G.A. Abakumov and C.G. Pierpont, *J. Am. Chem. Soc.*, **114**, 4220 (1992).
- [273] P.Y. Feng, X.H. Bu and N.F. Zheng, *Acc. Chem. Res.*, **38**, 293 (2005).
- [274] A. Aumüller, P. Erk, G. Klebe, S. Hünig, J.U. von Schütz and H.P. Werner, *Angew. Chem. Int. Ed.*, **25**, 740 (1986).
- [275] J.M. Williams, J.R. Ferraro and R.J. Thorn, *Organic Superconductors: Synthesis, Structure, Properties and Theory (Includes Fullerenes)*, Prentice Hall, Englewood Cliffs, NJ, 1991.
- [276] M. Kurmoo, A.W. Graham, P. Day, S.J. Coles, M.B. Hursthouse, J.L. Caulfield, J. Singleton, F.L. Pratt, W. Hayes, L. Ducasse and P. Guionneau, *J. Am. Chem. Soc.*, **117**, 12209 (1995).
- [277] E. Coronado, J.R. Galan-Mascaros, C.J. Gomez-Garcia and V. Laukhin, *Nature*, **408**, 447 (2000).
- [278] M.D. Allendorf, C.A. Bauer, R.K. Bhakta and R.J.T. Houk, *Chem. Soc. Rev.*, **38**, 1330 (2009).
- [279] M.P. Suh, Y.E. Cheon and E.Y. Lee, *Coord. Chem. Rev.*, **252**, 1007 (2008).
- [280] B.T.N. Pham, L.M. Lund and D.T. Song, *Inorg. Chem.*, **47**, 6329 (2008).
- [281] J. Pang, E.J.P. Marcotte, C. Seward, R.S. Brown and S.N. Wang, *Angew. Chem. Int. Ed.*, **40**, 4042 (2001).
- [282] Y.Q. Huang, B. Ding, H.B. Song, B. Zhao, P. Ren, P. Cheng, H.G. Wang, D.Z. Liao and S.P. Yan, *Chem. Commun.*, 4906 (2006).
- [283] W.H. Zhu, Z.M. Wang and S. Gao, *Inorg. Chem.*, **46**, 1337 (2007).
- [284] T.M. Reineke, M. Eddaoudi, M. Fehr, D. Kelley and O.M. Yaghi, *J. Am. Chem. Soc.*, **121**, 1651 (1999).
- [285] B.L. Chen, Y. Yang, F. Zapata, G.N. Lin, G.D. Qian and E.B. Lobkovsky, *Adv. Mater.*, **19**, 1693 (2007).
- [286] B.V. Harbuzaru, A. Corma, F. Rey, P. Atienzar, J.L. Jorda, H. Garcia, D. Ananias, L.D. Carlos and J. Rocha, *Angew. Chem. Int. Ed.*, **47**, 1080 (2008).
- [287] B.L. Chen, L.B. Wang, F. Zapata, G.D. Qian and E.B. Lobkovsky, *J. Am. Chem. Soc.*, **130**, 6718 (2008).
- [288] K.L. Wong, G.L. Law, Y.Y. Yang and W.T. Wong, *Adv. Mater.*, **18**, 1051 (2006).
- [289] Y.C. Qiu, Z.H. Liu, Y.H. Li, H. Deng, R.H. Zeng and M. Zeller, *Inorg. Chem.*, **47**, 5122 (2008).
- [290] B. Zhao, X.Y. Chen, P. Cheng, D.Z. Liao, S.P. Yan and Z.H. Jiang, *J. Am. Chem. Soc.*, **126**, 15394 (2004).
- [291] W. Liu, T. Jiao, Y. Li, Q. Liu, M. Tan, H. Wang and L. Wang, *J. Am. Chem. Soc.*, **126**, 2280 (2004).
- [292] E.Y. Lee, S.Y. Jang and M.P. Suh, *J. Am. Chem. Soc.*, **127**, 6374 (2005).

- [293] C.A. Bauer, T.V. Timofeeva, T.B. Settersten, B.D. Patterson, V.H. Liu, B.A. Simmons and M.D. Allendorf, *J. Am. Chem. Soc.*, **129**, 7136 (2007).
- [294] J.R. Salvador, F. Gu, T. Hogan and M.G. Kanatzidis, *Nature*, **425**, 702 (2003).
- [295] J. Arvanitidis, K. Papagelis, S. Margadonna, K. Prassides and A.N. Fitch, *Nature*, **425**, 599 (2003).
- [296] S. Margadonna, J. Arvanitidis, K. Papagelis and K. Prassides, *Chem. Mater.*, **17**, 4474 (2005).
- [297] A.C. McLaughlin, F. Sher and J.P. Attfield, *Nature*, **436**, 829 (2005).
- [298] A.W. Sleight, *Curr. Opin. Solid State Mater. Chem.*, **3**, 128 (1998).
- [299] J.S.O. Evans, *J. Chem. Soc., Dalton Trans.*, 3317 (1999).
- [300] M.G. Tucker, A.L. Goodwin, M.T. Dove, D.A. Keen, S.A. Wells and J.S.O. Evans, *Phys. Rev. Lett.*, **95**, 255501 (2005).
- [301] T.A. Mary, J.S.O. Evans, T. Vogt and A.W. Sleight, *Science*, **272**, 90 (1996).
- [302] S. Margadonna, K. Prassides and A.N. Fitch, *J. Am. Chem. Soc.*, **126**, 15390 (2004).
- [303] A.L. Goodwin and C.J. Kepert, *Phys. Rev. B: Condens. Matter*, **71**, 140301/1 (2005).
- [304] A.E. Phillips, A.L. Goodwin, G.J. Halder, P.D. Southon and C.J. Kepert, *Angew. Chem. Int. Ed.*, **47**, 1396 (2008).
- [305] A.L. Goodwin, K.W. Chapman and C.J. Kepert, *J. Am. Chem. Soc.*, **127**, 17980 (2005).
- [306] K.W. Chapman, P.J. Chupas and C.J. Kepert, *J. Am. Chem. Soc.*, **127**, 15630 (2005).
- [307] K.W. Chapman, P.J. Chupas and C.J. Kepert, *J. Am. Chem. Soc.*, **128**, 7009 (2006).
- [308] T. Prets, K.W. Chapman, G.J. Halder and C.J. Kepert, *Chem. Commun.*, 1857 (2006).
- [309] A.L. Goodwin, M. Calleja, M.J. Conterio, M.T. Dove, J.S.O. Evans, D.A. Keen, L. Peters and M.G. Tucker, *Science*, **319**, 794 (2008).
- [310] A.L. Goodwin, B.J. Kennedy and C.J. Kepert, *J. Am. Chem. Soc.*, **131**, 6334 (2009).
- [311] S.J. Hibble, A.M. Chippindale, A.H. Pohl and A.C. Hannon, *Angew. Chem. Int. Ed.*, **46**, 7116 (2007).
- [312] Y. Wu, A. Kobayashi, G.J. Halder, V.K. Peterson, K.W. Chapman, N. Lock, P.D. Southon and C.J. Kepert, *Angew. Chem. Int. Ed.*, **47**, 8929 (2008).
- [313] D. Dubbeldam, K.S. Walton, D.E. Ellis and R.Q. Snurr, *Angew. Chem. Int. Ed.*, **46**, 4496 (2007).
- [314] S.S. Han and W.A. Goddard, *J. Phys. Chem. C*, **111**, 15185 (2007).
- [315] J.L. Korcok, M.J. Katz and D.B. Leznoff, *J. Am. Chem. Soc.*, **131**, 4866 (2009).
- [316] A.L. Goodwin, D.A. Keen and M.G. Tucker, *Proc. Natl. Acad. Sci. USA*, **105**, 18708 (2008).
- [317] K.W. Chapman, G.J. Halder and P.J. Chupas, *J. Am. Chem. Soc.*, **130**, 10524 (2008).
- [318] K.W. Chapman and P.J. Chupas, *J. Am. Chem. Soc.*, **129**, 10090 (2007).
- [319] G.B. Gardner, D. Venkataraman, J.S. Moore and S. Lee, *Nature*, **374**, 792 (1995).
- [320] R.H. Baughman and D.S. Galvao, *Nature*, **365**, 735 (1993).
- [321] K.E. Evans, M.A. Nkansah, I.J. Hutchinson and S.C. Rogers, *Nature*, **353**, 124 (1991).

